

NO-A151 838

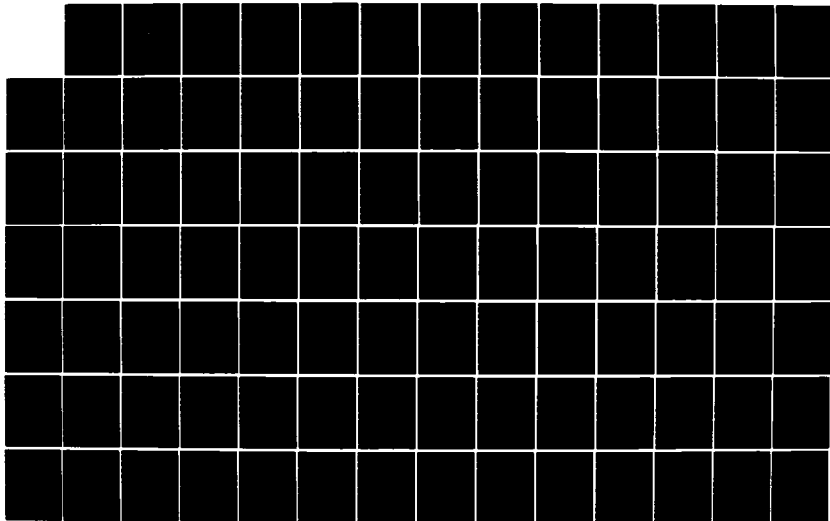
TURBULENCE EFFECTS ON A GLOW DISCHARGE AS DERIVED FROM
CONTINUITY AND ENERGY CONSIDERATIONS(U) NAVAL
POSTGRADUATE SCHOOL MONTEREY CA W R OKER SEP 84

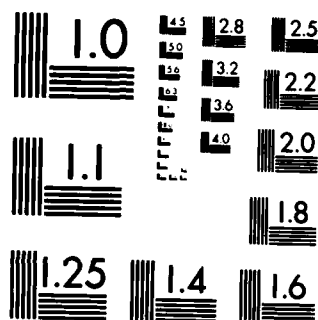
1/2

UNCLASSIFIED

F/G 20/4

NL





MICROCOPY RESOLUTION TEST CHART
NATIONAL BUREAU OF STANDARDS-1963-A

②

AD-A151 838

NAVAL POSTGRADUATE SCHOOL

Monterey, California



DTIC
ELECTE
APR 1 1985
S B D

THESIS

TURBULENCE EFFECTS ON A
GLOW DISCHARGE AS DERIVED FROM
CONTINUITY AND ENERGY CONSIDERATIONS

by

William R. Oker

September 1984

Thesis Advisor: Oscar Biblarz

Approved for public release; distribution unlimited

DTIC FILE COPY

85 03 14 028

UNCLASSIFIED

SECURITY CLASSIFICATION OF THIS PAGE (When Data Entered)

REPORT DOCUMENTATION PAGE		READ INSTRUCTIONS BEFORE COMPLETING FORM
1. REPORT NUMBER	2. GOVT ACCESSION NO.	3. RECIPIENT'S CATALOG NUMBER
4. TITLE (and Subtitle) Turbulence Effects on a Glow Discharge as Derived from Continuity and Energy Considerations		5. TYPE OF REPORT & PERIOD COVERED Master's Thesis September 1984
		6. PERFORMING ORG. REPORT NUMBER
7. AUTHOR(s) William R. Oker		8. CONTRACT OR GRANT NUMBER(s)
9. PERFORMING ORGANIZATION NAME AND ADDRESS Naval Postgraduate School Monterey, California 93943		10. PROGRAM ELEMENT, PROJECT, TASK AREA & WORK UNIT NUMBERS
11. CONTROLLING OFFICE NAME AND ADDRESS Naval Postgraduate School Monterey, California 93943		12. REPORT DATE September 1984
		13. NUMBER OF PAGES 98
14. MONITORING AGENCY NAME & ADDRESS (if different from Controlling Office)		15. SECURITY CLASS. (of this report) Unclassified
		15a. DECLASSIFICATION/DOWNGRADING SCHEDULE
16. DISTRIBUTION STATEMENT (of this Report) Approved for public release; distribution unlimited		
17. DISTRIBUTION STATEMENT (of the abstract entered in Block 20, if different from Report)		
18. SUPPLEMENTARY NOTES		
19. KEY WORDS (Continue on reverse side if necessary and identify by block number) Glow-To-Arc-Transition, Glow-Discharge, Turbulent Diffusion, Streamer-Breakdown, Arc Breakdown		
20. ABSTRACT (Continue on reverse side if necessary and identify by block number) Effects of a turbulent gas flow on the stability of a glow discharge are investigated. While it is known that turbulence affects the stability of glow discharges, the mechanism is not clear. Primarily, the problem lies in the very long character- istic times of turbulence phenomena when compared to the glow discharge instability times.		

DD FORM 1 JAN 73 1473

EDITION OF 1 NOV 65 IS OBSOLETE

S N 0102-LF-014-6601

UNCLASSIFIED

1 SECURITY CLASSIFICATION OF THIS PAGE (When Data Entered)

UNCLASSIFIED

SECURITY CLASSIFICATION OF THIS PAGE (When Data Entered)

#20 - ABSTRACT - (CONTINUED)

A mathematical model is developed which is solved numerically for the ambipolar diffusion and an overall energy equation in an unsteady, cylindrical coordinate system. Strong perturbations of the electric field are introduced which disturb an otherwise stable configuration and the effects of turbulence on the time evolution of the perturbation are observed.

It is shown that the modification of the ambipolar diffusion coefficient and the thermal conductivity is a reasonably sufficient model to introduce the turbulence effects. It is found that the charged particle density is effectively the sole source of heating in the gaseous environment of the discharge. It is then shown that turbulence acts to suppress the temperature instability introduced by the discharge streamer. *Augmentation of field*

UNCLASSIFIED

SECURITY CLASSIFICATION OF THIS PAGE (When Data Entered)

Approved for public release; distribution unlimited

Turbulence Effects on a
Glow Discharge as Derived from
Continuity and Energy Considerations

by

William R. Oker
Lieutenant Commander, United States Navy
B.S., California State Polytechnic University, 1972

Submitted in partial fulfillment of the
requirements for the degree of

MASTER OF SCIENCE IN AERONAUTICAL ENGINEERING

from the

NAVAL POSTGRADUATE SCHOOL
September 1984

Author:

William R. Oker

William R. Oker

Approved by:

Oscar Biblarz

Oscar Biblarz, Thesis Advisor

M. F. Platzer

M. F. Platzer, Chairman,
Department of Aeronautics

J. N. Dyer

J. N. Dyer,
Dean of Science and Engineering

ABSTRACT

Effects of a turbulent gas flow on the stability of a glow discharge are investigated. While it is known that turbulence affects the stability of glow discharges, the mechanism is not clear. Primarily, the problem lies in the very long characteristic times of turbulence phenomena when compared to the glow discharge instability times.

A mathematical model is developed which is solved numerically for the ambipolar diffusion and an overall energy equation in an unsteady, cylindrical coordinate system. Strong perturbations of the electric field are introduced which disturb an otherwise stable configuration and the effects of turbulence on the time evolution of the perturbation are observed.

It is shown that the modification of the ambipolar diffusion coefficient and the thermal conductivity is a reasonably sufficient model to introduce the turbulence effects. It is found that the charged particle density is effectively the sole source of heating in the gaseous environment of the discharge. It is then shown that turbulence acts to suppress the temperature instability introduced by the discharge streamer.

TABLE OF CONTENTS

I.	INTRODUCTION -----	11
II.	ANALYSIS -----	15
	A. THE CONTINUITY EQUATION -----	15
	B. THE ENERGY EQUATION -----	19
	C. SOLVING THE EQUATIONS -----	22
	D. MODELING THE STREAMER -----	29
III.	RESULTS AND DISCUSSION -----	31
	A. NON-IONIZED ENVIRONMENT CASE -----	31
	B. IONIZED ENVIRONMENT CASE -----	46
IV.	CONCLUSIONS AND RECOMMENDATIONS -----	72
	LIST OF REFERENCES -----	75
	APPENDIX A: THE CHARGE PROGRAM -----	76
	APPENDIX B: HP-41 PROGRAM -----	94
	BIBLIOGRAPHY -----	97
	INITIAL DISTRIBUTION LIST -----	98



Accession For	
NTIS STAR	<input checked="" type="checkbox"/>
DTIC TAB	<input type="checkbox"/>
Unannounced	<input type="checkbox"/>
Justification	
Availability Codes	
Avail and/or	
Dist	Special
A-1	

LIST OF FIGURES

2.1	Streamer Geometry -----	17
2.2	Relevant Properties of Nitrogen -----	20
3.1	Charged Particle Density Profile in Laminar Flow -----	32
3.2	Charged Particle Density Profile in Turbulent Flow -----	34
3.3	Gamma vs Time in Laminar Flow -----	36
3.4	Gamma vs Beta -----	37
3.5	Gamma vs Beta for Streamer Tube -----	39
3.6	Temperature Profile for $E = 4.0E4$ V/m -----	40
3.7	Temperature Profile for $E = 1.0E6$ V/m -----	42
3.8	Temperature Profile for $E = 2.0E6$ V/m -----	43
3.9	Temperature Profile for $E = 4.0E6$ V/m -----	44
3.10	Temperature Profile for $E = 8.0E6$ V/m -----	45
3.11	Temperature Profile for $No = 3.125E19$ /m ³ -----	47
3.12	Temperature Profile for $No = 3.125E20$ /m ³ -----	48
3.13	Temperature Profile for $BAMIN = 800$ -----	50
3.14	Temperature Profile for $BAMIN = 3$ -----	51
3.15	Temperature Profile for $BAMIN = 1$ -----	52
3.16	Temperature Profile for $BAMIN = 0.4$ -----	53
3.17	Charged Particle Density Profile with Ionization Term -----	56
3.18	Temperature Profile in Turbulent Flow -----	57
3.19	Temperature Profile with Streamer on 5 TR -----	59
3.20	Temperature Profile with Streamer on 10 TR -----	60

3.21	Temperature Profile with Streamer on 15 TR	-----	61
3.22	Temperature Profile with Streamer on 20 TR	-----	62
3.23	Temperature Profile with Streamer on 25 TR	-----	63
3.24	Temperature Profile with Streamer on 30 TR	-----	64
3.25	Temperature Profile with Streamer on 35 TR	-----	65
3.26	Temperature Profile with Streamer on 40 TR	-----	66
3.27	Temperature Profile with Streamer on 45 TR	-----	67
3.28	Temperature Profile with Streamer on 50 TR	-----	68
3.29	Temperature Profile with Streamer on 5 TR	-----	70
3.30	Temperature Profile with Streamer on 8 TR	-----	71

LIST OF SYMBOLS

A	=	area
α	=	$\alpha_3 n_0 / \alpha_2$
α_2	=	two-body recombination coefficient
α_3	=	three-body recombination coefficient
β	=	inverse turbulence parameter due to ambipolar diffusion
β_A	=	inverse turbulence parameter due to thermal conductivity
D_a	=	ambipolar diffusion coefficient
e	=	internal energy, or elementary electron charge
E, E_0	=	electric field strength, initial value
G	=	conductance
I	=	current
j	=	current density
K	=	thermal conductivity
k	=	Boltzman's constant
l	=	length of streamer (or distance between electrodes)
m_e	=	electron mass
μ_e	=	electron mobility
n, n_0	=	charged particle density, initial value
n_c	=	n value on streamer centerline
\hat{n}	=	non-dimensionalized n
n_e	=	number of electrons
N	=	total number of particles
ν_i	=	ionization coefficient

ν_e = electron collision frequency
 Ω = resistance
 P = pressure
 q = heat flux
 r, r_0 = streamer channel radius, initial value
 \hat{r} = non-dimensionalized radius
 ρ = density
 σ, σ_0 = conductivity, initial value
 T, T_0 = temperature, initial value
 \hat{T} = non-dimensionalized temperature
 τ_R = characteristic recombination time
 TR = same as τ_R
 τ_A = characteristic time for energy equation
 t, t_0 = time, initial value
 \hat{t} = non-dimensionalized time
 t_A = t associated with τ_A
 U = gas flow velocity
 v_d = electron drift velocity
 V = voltage
 Z = electric field perturbation parameter for continuity equation
 Z_A = "Z" for energy equation

ACKNOWLEDGEMENTS

I would like to express my sincere appreciation to Professor Oscar Biblarz, whose assistance and encouragement were vital to this research.

I wish to dedicate this thesis to my wife, Barbara. Without her constant love, support, and understanding, this work would not have been possible.

I. INTRODUCTION

If a gas such as nitrogen or argon, or a mixture of gases such as air, is subjected to an electrical potential, a sequence of phenomena take place as a result of a continuously increasing applied voltage and/or current. Initially, for a small voltage, a very weak current on the order of 0.1 picoamperes develops. This current will increase slightly with increasing voltage until all the naturally occurring charge carriers are being utilized. A current saturation condition now prevails until the applied voltage reaches about 6 kV in air at which time a further voltage rise rapidly increases the current flow to about one picoampere. This is referred to as the Townsend Discharge Region and it is due to new charge carriers being created by collisions between the highly energetic electrons (fast moving) and the neutral (slow moving) atoms. This process can have several effects on the individual gas molecules. Essentially, it can excite them, dissociate them, and/or ionize them. This ionization effect is higher for lower gas pressures since the farther the electron travels between collisions the higher will be its kinetic energy which is imparted by the acceleration produced by the applied electric field. When the electron's energy is greater than that required for ionization of the neutral gas particles the collisions will

produce additional electrons which in turn gain energy, produce collisions, and therefore, increase the total number of electrons present. This process is called an electron avalanche.

From this point, slight increases in voltage produce current increases of several orders of magnitude at which time the current becomes self sustaining. Reducing the external circuit resistance now increases the current flow and a steady glow is produced in the gas. This glow-discharge is the familiar phenomenon which occurs in neon lights and has other practical applications such as a pumping scheme for gas lasers.

Finally, when the current is increased still further, a highly ionized channel is formed which collapses the glow. If there is sufficient current carrying capacity in the external circuit a steady current is established which represents a plasma state called an arc.

A full understanding of the arcing mechanism is difficult due to the extremely short formation times involved. However, since delaying the point of transition to arcing is a highly practical problem, a method for modeling it is needed. A blend of theory and experiment is usually required. Such a model could then be used to study the effects of the arc on and by its environment.

It has been observed that this glow-to-arc transition can be delayed by utilizing gas dynamic stabilization

techniques in flowing gas systems [Ref. 1]. The purpose of this work is to establish the extent of fluid dynamic stabilization that results from the introduction of varying levels of fluid dynamic turbulence into the flow. It will be shown that this method has beneficial effects on the stability of the glow discharge process and on the temperature distribution in the gas produced by the presence of discharge streamers. For further discussion and background information relating to ionization and the breakdown processes refer to any standard reference in the field or to Wallace, R.J. [Ref. 2].

An introductory skill level in atomic physics plus fundamental proficiencies in mechanics, electrical principles and numerical analysis should provide the reader with adequate preparation for understanding this material.

The principles discussed here have many practical engineering applications. For maximum power output of an electrically pumped gas laser, such as a carbon dioxide laser, the glow discharge must be held essentially at the limit of arcing. Since turbulent flows tend to delay this glow-to-arc transition, the laser can be allowed to operate at either the highest possible power level or with a greater margin of safety at lower power levels. Another application where a stabilized high frequency electrical spark discharge could be used as a means for injecting heat into a propulsive duct (like a pulsejet) has been suggested by C.E. Tharratt [Ref. 3].

This type of a device is theoretically capable of unlimited thrust. It would also have a low specific fuel consumption and could operate outside the audible range. The possibility of nearly silent operation would be highly advantageous as an aircraft propulsion device for the future.

Two major cases will be discussed. The first case concerns the behavior of a highly transient discharge in a non-ionized gaseous environment such as the lightning discharge. This first case concerns a pre-glow discharge type phenomenon since the streamer propagates in a non-ionized medium. However, it serves to establish the effects of turbulence in a simpler situation in order to form a starting place for this research. The second case will look at discharge streamers in a partially ionized gas which might be used for the pumping mechanism of a gas laser. The method of approach to these problems will be developed in the next chapter where a mathematical model will be presented. The governing partial differential equations for the model presented will be solved by numerical integration techniques utilizing a computer. A working Fortran program is presented which can be used to investigate a wide variety of the aspects of this problem. Significant results are then presented in graphical format to demonstrate the stabilizing features of the turbulent flow.

II. ANALYSIS

A. THE CONTINUITY EQUATION

Highly ionized channels which develop at the final stages of a glow discharge just prior to arc breakdown are called streamers. The transition to arcing is then often due to streamer-breakdown. It should be noted here that the type of streamers to be analyzed are the non-self-sustaining discharge streamers that precede the arc, rather than the electron avalanche (onset streamers) type that occur earlier in the glow discharge phenomena.

Streamers are seen to issue from either electrode and appear always to precede the breakdown. These streamers propagate virtually instantaneously for our purposes as an ultrafast ionization wave. They consist of a partially ionized plasma column for which the conductivity is dependent directly on the charged particle density within the streamer [Ref. 4]. It will be shown that the collisions made by the charged particles within these streamers are the main source of heating of the surrounding gas. The value of this charged particle density may be determined by the application of the following continuity equation to the breakdown process.

$$\frac{\partial n}{\partial t} = \frac{D_a}{r} \frac{\partial}{\partial r} \left(r \frac{\partial n}{\partial r} \right) - U \frac{\partial n}{\partial r} - \alpha_2 n^2 - \alpha_3 n^3 \quad (2.1)$$

Equation (2.1) gives the time rate of change of the charged particle density, n , as a function of radial position, r , and time, t , for the decaying streamer. It is written in cylindrical coordinates due to the natural form of the streamer. A schematic drawing of the streamer geometry is depicted in Figure 2.1. The right hand side (RHS) of Equation (2.1) consists of three classes of terms. The first term represents the effect of diffusion due to the high density gradient within the plasma channel. D_a is the ambipolar diffusion coefficient. This ambipolar diffusion results in the electrons and ions diffusing out of the original channel at essentially the same rate. Briefly, the lighter electrons having higher thermal velocities leave the plasma ahead of the slower, heavier ions. This produces a local positive space charge which retards the loss of electrons and accelerates the loss of the ions. The net effect is that the ambipolar diffusion coefficient is approximately twice the diffusion coefficient of the ions alone [Ref. 4].

Next consider terms 3 and 4 of the RHS of Equation (2.1) which represent two and three-body recombination respectively. Recombination is a de-ionization process which is then responsible here for the reduction in conductivity of the partially ionized gas. These processes occur when an electron and an ion collide at relatively low velocity and recombine to form a neutral atom. In order to conserve linear momentum a third body must be present. In two-body recombination

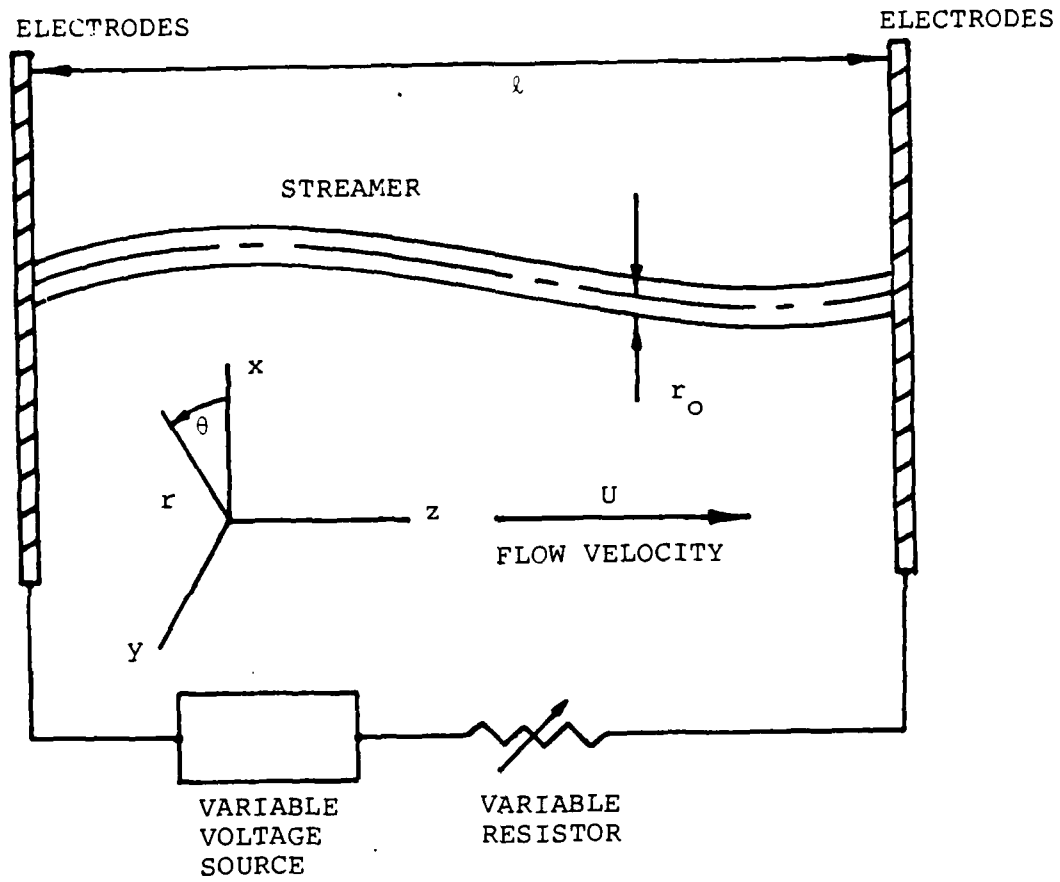


Figure 2.1. Streamer Geometry

this third body is a photon and, therefore, this process is sometimes called radiative recombination. For three-body recombination the third body is usually an ion or neutral atom [Ref. 4]. Due to the large complexity of electron loss mechanisms accurate values for the recombination coefficients are difficult to obtain. The values used in this thesis will be discussed in the next subsection.

The second term on the RHS is the convection term. This term is neglected since the characteristic time of convection (length/flow velocity) is much less than the characteristic recombination times associated with terms 3 and 4 [Ref. 2].

While the convection term in Equation (2.1) can be neglected, the diffusion term cannot since the diffusion coefficient D_a can increase by about three orders of magnitude between laminar and turbulent flow [Ref. 2]. This will cause the characteristic diffusion time to be on the same order of magnitude as the recombination time and some relationship will exist between diffusion and recombination which will affect the charged particle density distribution, n , in space and time.

Once Equation (2.1) is solved for $n(r,t)$ the resulting distribution profile can be integrated to determine a conductance of the decaying streamer as a function of the streamer radius and time. This can be accomplished under varying turbulence level conditions by changing the effective value of the diffusion coefficient.

Equation (2.1) describes the lightning-discharge type phenomenon in a non-ionized medium. A more interesting situation is the case of the streamer as it appears in an ionized-sustainer discharge for the pumping of a gas laser [Ref. 5]. For this case, Equation (2.1) may be written as,

$$\frac{\partial n}{\partial t} - \frac{D_a}{r} \frac{\partial}{\partial r} \left(r \frac{\partial n}{\partial r} \right) = v_i n - \alpha_2 n^2 - \alpha_3 n^3 \quad (2.2)$$

where now a new first term is added to the RHS which represents a production of electrons and ions. The ionization coefficient, v_i , is a function of the sustainer E/N and can be determined from Figure 2.2. The electric field referred to here is an existing axial electric field, that is, the "pumping field" that maintains the glow. Equations (2.1) and (2.2) are non-linear partial differential equations which will be solved numerically by the use of a finite difference approximation scheme.

B. THE ENERGY EQUATION

In addition to the continuity equation, a suitable energy equation must be considered in order to describe the temperature distribution introduced into the gas by the glow discharge streamer. For thermal stability to exist, a balance must be created such that the time rate of change of the internal energy is zero because the loss of heat through thermal conductivity and the addition of energy from Ohmic

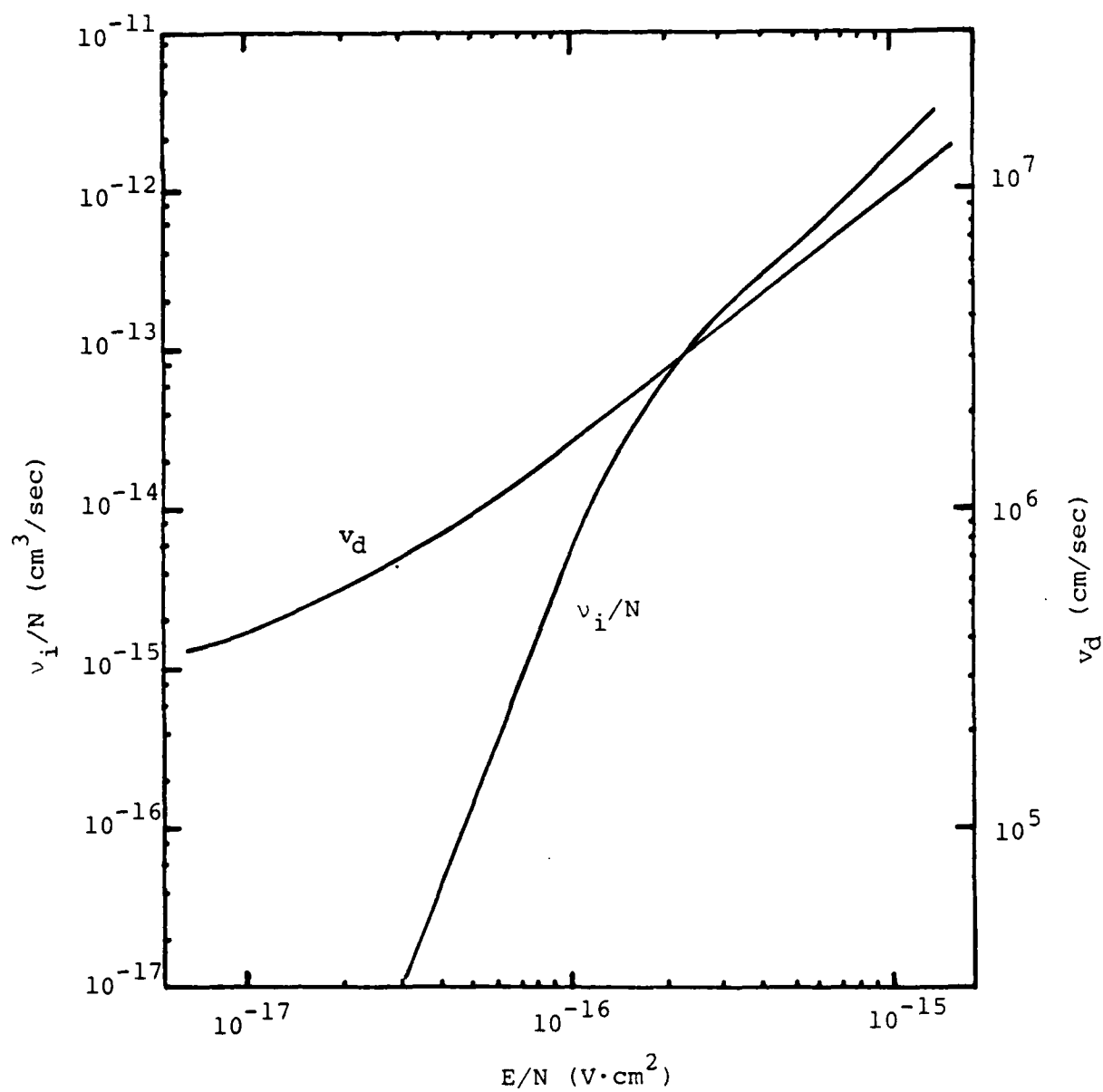


Figure 2.2. Relevant Properties of Nitrogen

heating must balance each other. The following equation represents this relationship.

$$\rho \frac{De}{Dt} = \vec{E} \cdot \vec{j} - \nabla \cdot \vec{q} \quad (2.3)$$

The first term on the RHS of Equation (2.3) represents Joule or Ohmic heating where, \vec{E} , is the electric field strength and, \vec{j} , is the current density. The second term is the heat flux loss due to thermal conductivity and radiation. The total derivative,

$$\frac{De}{Dt} = \frac{\partial e}{\partial t} + v_r \frac{\partial e}{\partial r} + v_\theta \frac{\partial e}{\partial \theta} + v_z \frac{\partial e}{\partial z} \quad (2.4)$$

reduces to, $\frac{\partial e}{\partial t}$, since the model under consideration here allows for conduction only in the "z" direction. It is further assumed that the change of the internal energy along the length of the streamer is small, the radiation emitted primarily perpendicular to the streamer centerline has a negligible effect and, due to the short characteristic times involved, the heating occurs at an essentially constant volume. With these assumptions in mind, Equation (2.3) becomes,

$$\rho C_v \frac{\partial T}{\partial t} - K \nabla^2 T = \sigma E_z^2 \quad (2.5)$$

where, ρ , is the gas density, σ , is the electrical conductivity of the plasma (recalling that $j = \sigma E_z$) and K is the

thermal conductivity. Equation (2.5) gives the temperature, T , as a function of the radius and time.

The conductivity, σ , is given by,

$$\sigma = e n_e \mu_e \quad (2.6)$$

where, e , is the elementary electronic charge in coulombs, n_e , is the number of electrons and, μ_e , is the electron mobility. The mobility is also a function of E/N and is defined as the ratio of the electron drift velocity, v_d , to the applied external electric field. The value of v_d is given in Figure 2.2 as a function of E/N .

It will be shown later that for the σE_z^2 term from Equation (2.5), E_z is essentially constant and since σ is directly proportional to n the solution of Equation (2.2) represents the single source of heating that drives the temperature distribution obtained from Equation (2.5). The consequence of this is that a mathematical model describing the temporal and spatial characteristics of the streamer can now be developed. Furthermore, the effects of turbulence as a stabilizing medium can then be studied since the thermal conductivity, K , and the ambipolar diffusion coefficient, D_a , are the only parameters affected by turbulence in Equations (2.1), (2.2) and (2.5).

C. SOLVING THE EQUATIONS

An effective means of generalizing a problem such as this is to non-dimensionalize the equations. To begin then,

after some algebraic manipulation, Equation (2.1) can be written in the form,

$$\frac{1}{\alpha_2 n_0} \frac{\partial \hat{n}}{\partial t} - \left[\frac{D_a}{n_0 \alpha_2 r_0^2} \right] \frac{\partial}{\partial \hat{r}} \left(\hat{r} \frac{\partial \hat{n}}{\partial \hat{r}} \right) = -\hat{n}^2 - \frac{\alpha_3 n_0}{\alpha_2} \hat{n}^3 \quad (2.7)$$

where $\hat{n} = n/n_0$ and $\hat{r} = r/r_0$. " n_0 " and " r_0 " are the initial values for the charged particle density and the streamer radius. The following additional definitions will prove useful in this model,

$$\beta \equiv \frac{\alpha_2 n_0 r_0^2}{D_a} \quad (2.8)$$

$$\alpha \equiv \frac{\alpha_3 n_0}{\alpha_2} \quad (2.9)$$

$$\hat{t} \equiv \frac{t}{\tau_R} \quad (2.10)$$

The parameter, β , is an inverse measure of the turbulence level since the ambipolar diffusion coefficient is smaller in laminar flow (large β) and larger in a turbulent flow (small β). If one neglects the diffusion term in Equation (2.1), then for two-body recombination, direct integration yields,

$$n = \frac{n_0}{1 + \alpha_2 n_0 t} \quad (2.11)$$

This ion loss formula [Ref. 2] then shows that the characteristic recombination time, τ_R , is simply $1/\alpha_2 n_0$.

Incorporating the above definitions allows Equation (2.7) to be written in the non-dimensionalized form,

$$\frac{\partial \hat{n}}{\partial \hat{t}} - \frac{1}{\beta} \frac{\partial}{\partial \hat{r}} \left(\hat{r} \frac{\partial \hat{n}}{\partial \hat{r}} \right) = -\hat{n}^2 - \alpha \hat{n}^3 \quad (2.12)$$

which lends itself to a numerical solution by substituting the appropriate finite difference approximation formula [Ref. 6] for the differentials. After some manipulation, Equation (2.12) can be approximated by,

$$\hat{n}_{i,j+1} = \left\{ \Delta \hat{t} \left[\frac{1}{\beta} (A + B) - C \right] \right\} + \hat{n}_{i,j} \quad (2.13)$$

where,

$$A = \frac{1}{\Delta \hat{r}^2} (\hat{n}_{i+1,j} - 2\hat{n}_{i,j} + \hat{n}_{i-1,j}) \quad (2.14)$$

$$B = \frac{1}{2\hat{r}\Delta \hat{r}} (\hat{n}_{i+1,j} - \hat{n}_{i-1,j}) \quad (2.15)$$

$$C = (\hat{n}_{i,j}^2 + \alpha \hat{n}_{i,j}^3) \quad (2.16)$$

In this scheme, 'i' represents position perpendicular to the streamer centerline and 'j' represents relative position in time after some initial condition. Equations (2.13) through (2.16) form the basic algorithm used by the Fortran program discussed in Appendix A.

The accuracy of the charged particle density obtained by this type of differencing scheme depends on the step sizes Δt and Δr . The steps must be smaller than the smallest characteristic time of the phenomena described. Therefore, Δt is taken as 0.1 or in real time $\tau_R/10$ [Ref. 6]. Primarily for programming convenience, Δr is also taken as 0.1. Additionally, the value of β is limited by the following stability criterion [Ref. 2].

$$\beta > \frac{2\Delta t}{\Delta r^2} \quad (2.17)$$

Returning to Equation (2.2), it is seen that the addition of the ionization term to the RHS requires a modification to Equation (2.16) which now becomes,

$$C_1 = [\hat{n}_{i,j}^2 + \alpha \hat{n}_{i,j}^3 - \hat{n}_{i,j}] \quad (2.18)$$

Equation (2.5) can be non-dimensionalized in a similar manner by writing it in the form,

$$\frac{T_O}{\tau_A} \frac{\partial \hat{T}}{\partial \hat{t}_A} - \left[\frac{KT_O}{\rho C_V r_O^2} \right] \frac{1}{\hat{r}} \frac{\partial}{\partial \hat{r}} \left[\hat{r} \frac{\partial \hat{T}}{\partial \hat{r}} \right] = \frac{\sigma E_z^2}{\rho C_V} \quad (2.19)$$

where τ_A is defined as,

$$\tau_A \equiv \frac{T_O \rho C_V}{\sigma_O E_{z_O}^2} \quad (2.20)$$

A check of Equation (2.20) reveals that τ_A has the units of seconds and, therefore, is a characteristic time for the energy equation. If one now defines the following additional relations,

$$\hat{t}_A \equiv \frac{t}{\tau_A} \quad (2.21)$$

$$\hat{T} \equiv \frac{T}{T_0} \quad (2.22)$$

$$\beta_A \equiv \frac{\sigma E_{z0}^2 r_0^2}{KT_0} \quad (2.23)$$

then, it can be shown that, Equation (2.19) becomes the following non-dimensional relation,

$$\frac{\partial \hat{T}}{\partial \hat{t}_A} - \frac{1}{\beta_A \hat{r}} \frac{\partial}{\partial \hat{r}} \left(\hat{r} \frac{\partial \hat{T}}{\partial \hat{r}} \right) = \frac{\sigma}{\sigma_0} \left(\frac{E_z^2}{E_{z0}^2} \right) \quad (2.24)$$

where, T_0 , is the initial temperature, which for this work, is taken as 300° Kelvin. It should be clear here that, β_A , is now a non-dimensional parameter whose value depends only on the thermal conductivity, K . This parameter then serves the same function for the energy equation as does β for the continuity equation, that is, it allows the influence of turbulence to be introduced into the model. The value of the electric field strength, E_z , from the RHS of Equation (2.24) can be estimated by assuming that the initial value of the externally applied field, E_0 , is given by [Ref. 8],

$$E_o = E + \frac{I\Omega}{\ell} \quad (2.25)$$

A reasonable value for Ω/ℓ might be on the order of 10,000 Ω/m , for which Equation (2.25) becomes,

$$E_o = E[1 + \frac{I}{E}(10,000)] \quad (2.26)$$

where I/E for the streamer can be shown to be,

$$\frac{I}{E} = \frac{e(\mu_e N)}{N} \int_0^r 2\pi r n_e dr \quad (2.27)$$

and,

$$N = \frac{P}{kT} \quad (2.28)$$

"N" is the total number of particles present in the gas at a pressure, P, and a temperature, T. The Boltzman constant is $k = 1.38\text{E-}23 \text{ J/}^\circ\text{K}$. The integral in Equation (2.27) is a measure of the conductance of the streamer and is evaluated in Chapter III by integrating the charged particle density distribution obtained from Equation (2.1). The initial value of this integral is simply $\pi n_o r_o^2$. Using estimates of n_o and r_o to be $3.125\text{E}18 \text{ m}^{-3}$ and $4.0\text{E-}4 \text{ m}$ respectively [Ref. 7], Equation (2.26) can be solved for E_z becoming,

$$E_{z_0} = \frac{E_0}{1 + 0.0006} \approx E_0 \quad (2.29)$$

where the value of $\mu_e N$ in Equation (2.27) can be obtained from reference tables to be $5.257E24 \text{ (v-m-s)}^{-1}$ for nitrogen. Results to be discussed in Chapter III show that the value of the integral drops rapidly to a small and nearly steady value (on the order of 0.01) such that the denominator of Equation (2.29) approaches unity in very short times.

The results of the previous paragraph then show that the RHS of Equation (2.24) is simply \hat{n} since σ/σ_0 is $(n_e \mu_e / n_0 \mu_e)$ and $E_z^2/E_{z_0}^2$ is approximately one. So now finally, Equation (2.24) can be written as,

$$\frac{\partial \hat{T}}{\partial \hat{t}_A} - \frac{1}{\beta_A \hat{r}} \frac{\partial}{\partial \hat{r}} \left[\hat{r} \frac{\partial \hat{T}}{\partial \hat{r}} \right] = \hat{n} \quad (2.30)$$

Equation (2.30) then shows that the temperature distribution due to the presence of the streamer is affected only by the charged particle density.

As for the continuity equations, Equation (2.30) can be solved by introducing the appropriate finite difference formula as follows (after some rearranging of terms),

$$\hat{T}_{i,j+1} = \Delta \hat{T} \left[\frac{1}{\beta_A} (A+B) + n_{i,j} \right] + \hat{T}_{i,j} \quad (2.31)$$

where,

$$A = \frac{1}{\Delta \hat{r}^2} [\hat{T}_{i+1,j} - 2\hat{T}_{i,j} + \hat{T}_{i-1,j}] \quad (2.32)$$

and,

$$B = \frac{1}{2\hat{r}\Delta \hat{r}} [\hat{T}_{i+1,j} - \hat{T}_{i-1,j}] \quad (2.33)$$

The Fortran program discussed in Appendix A solves Equation (2.31) simultaneously with Equation (2.1) or (2.2) depending on the case being considered by using the new value of \hat{n} calculated from each step as an input to the calculation of the new temperature value. The time step for the temperature calculation is adjusted such that the real time step for the two equations is equal.

D. MODELING THE STREAMER

The results of Chapter III show that appropriate selection of the controlling parameters for Equations (2.2) and (2.30) will produce a stable system in space and time. Then the question is: what effect does the momentary appearance of a streamer have on this stable situation? If a local perturbation of the electric field occurs, then the ionization coefficient will momentarily be raised which will in turn raise the charged particle density in the region of the perturbation. Figure 2.2 provides the data for estimating the magnitude of this perturbation by noting the relative increase in E/N for a corresponding increase in v_i/N . The

ratio of these values can then be used to determine a simple multiplier (labelled Z and Z_A) for the \hat{n} terms appearing on the RHS of Equations (2.2) and (2.30) to simulate the effect of the streamer. Therefore, one can write,

$$\frac{\partial \hat{n}}{\partial \hat{t}} - \frac{1}{\beta_A \hat{r}} \frac{\partial}{\partial \hat{r}} \left(\hat{r} \frac{\partial \hat{n}}{\partial \hat{r}} \right) = Z \hat{n} - \hat{n}^2 - \alpha \hat{n}^3 \quad (2.34)$$

and

$$\frac{\partial \hat{T}}{\partial \hat{t}_A} - \frac{1}{\beta_A \hat{r}} \left(\hat{r} \frac{\partial \hat{T}}{\partial \hat{r}} \right) = Z_A \hat{n} \quad (2.35)$$

where Z and Z_A are the multipliers discussed. For the finite difference approximations, these two additions are easily handled for Equations (2.2) and (2.30) respectively, as follows.

$$C_2 = [\hat{n}_{i,j}^2 - \alpha \hat{n}_{i,j}^3 - Z_i \hat{n}_{i,j}] \quad (2.36)$$

$$\hat{T}_{i,j+1} = \Delta \hat{t} \left[\frac{1}{\beta_A} (A+B) + Z_A \hat{n}_{i,j} \right] + \hat{T}_{i,j} \quad (2.37)$$

The Fortran program incorporates this concept by utilizing a separate subroutine called "STREMR" which is identical to the subroutine "DENSTY" except for the addition of Equations (2.36) and (2.37). In this scheme then, the streamer is modeled by calling up this subroutine when desired and then observing the reaction of the system over time.

III. RESULTS AND DISCUSSION

A. NON-IONIZED ENVIRONMENT CASE

In this section the effects of turbulence on the streamer in a non-ionized environment are considered. Equation (2.12) applies to this situation for which Figure 3.1 shows a typical plot of the charged particle density versus radial position perpendicular to the centerline in a fully laminar flow. Note that the abscissa and the ordinate are expressed in the non-dimensional coordinates of $\hat{r} = r/r_0$ and $\hat{n} = n/n_0$, respectively. There are five curves plotted which show the charged particle density distribution profile from the initial conditions at time zero in steps as specified in the legend to the profile at 3000 recombination times (TR). "TR" is the computer's version of " τ_R " and will be used here in the text. Now, for this plot, and except for Figures 3.11 and 3.12, for all the figures in this section, $n_0 = 3.125E18 \text{ m}^{-3}$, and $\alpha_2 = 2.0E-12 \text{ m}^3/\text{sec}$ [Ref. 7]. These values then equate to a recombination time of 0.16 microsecond, and so, 1000TR is equivalent to 0.16 millisecond in real time.

In the laminar case depicted in Figure 3.1 it is clearly seen that the centerline charged particle density drops off in time in accordance with Equation (2.11) which in non-dimensional form would be,

$$\hat{n}_c = \frac{1}{1 + \hat{t}} \quad (3.1)$$

CHARGED PARTICLE DENSITY PROFILE

IN LAMINAR FLOW

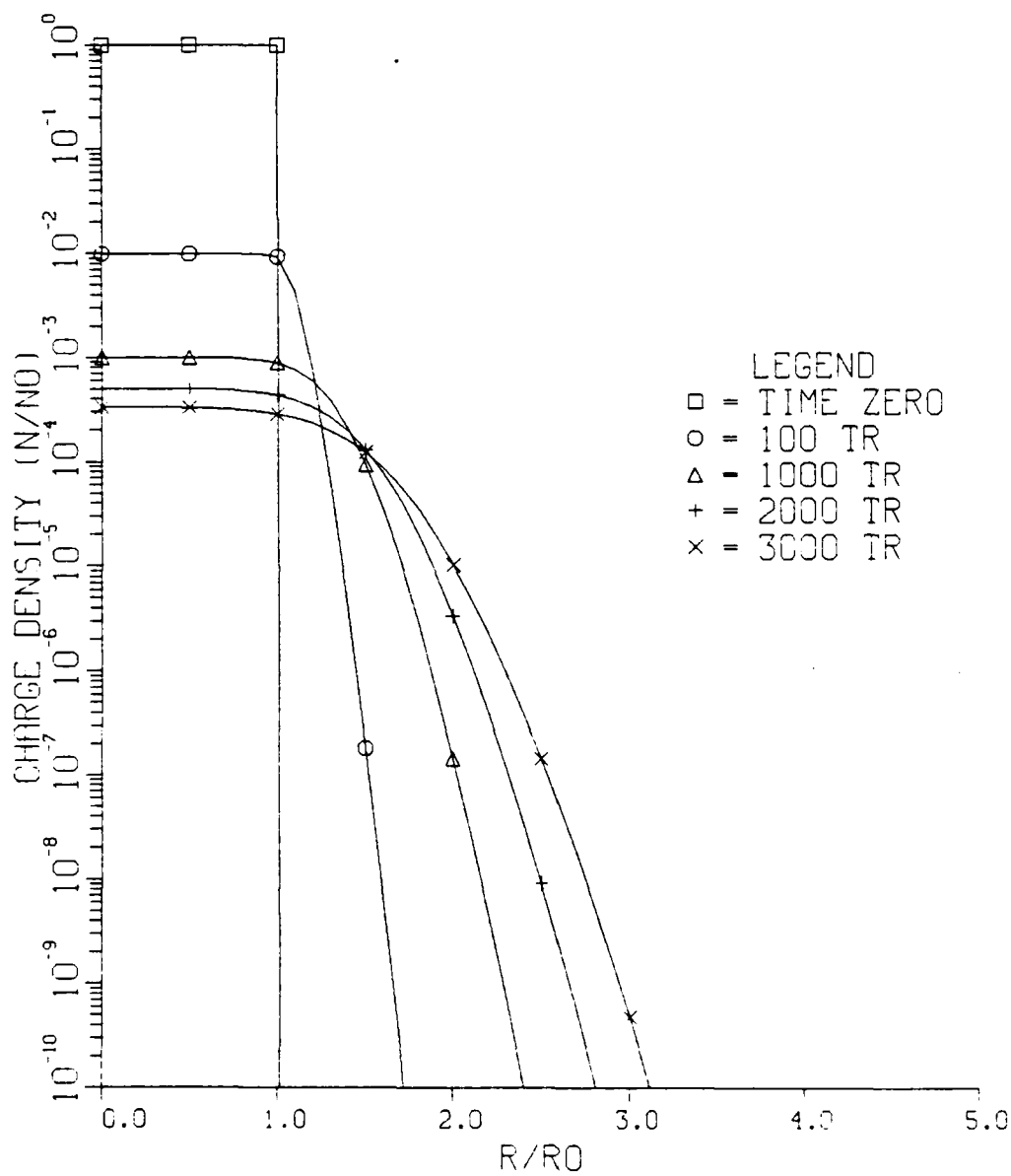


FIGURE 3.1

For example, at 1000TR, $\hat{n}_c = 1.0E-3$. This decay is due primarily to recombination only since, in this case, $\beta = 50,000$, and therefore, the diffusion term becomes very small. For longer times, diffusion comes into play and some spreading of the charge profile is seen.

Figure 3.2 shows the effect of introducing increasing amounts of turbulence into the flow. This plot compares the different charged particle profiles as they would appear at 0.32 msec for β values of 50 (fully turbulent), 500, 5000 and 50,000 (fully laminar). Note that the 2000TR curve from Figure 3.1 is identical to the $\beta = 50,000$ curve in Figure 3.2. The effect of the turbulence is clearly seen to spread out the profile and to lower \hat{n} on the centerline as well [Ref. 2].

As was mentioned previously, the conductance of the decaying streamer can be determined by integrating the charged particle density over the radius. This can be derived by "inverting" Ohm's law and introducing the conductivity expression for a partially ionized plasma for which the current can now be expressed as [Ref. 4],

$$I = GV = \left(\frac{\sigma A}{l}\right)V = \left(\frac{e^2 n_e A}{m_e v_e l}\right)V \quad (3.2)$$

where G is the conductance, or the reciprocal of the resistance, in the familiar relation, $V = IR$. ' σ ' is the conductivity, ' A ' the cross-sectional area and ' l ' is the

CHARGED PARTICLE DENSITY PROFILE
IN TURBULENT FLOW

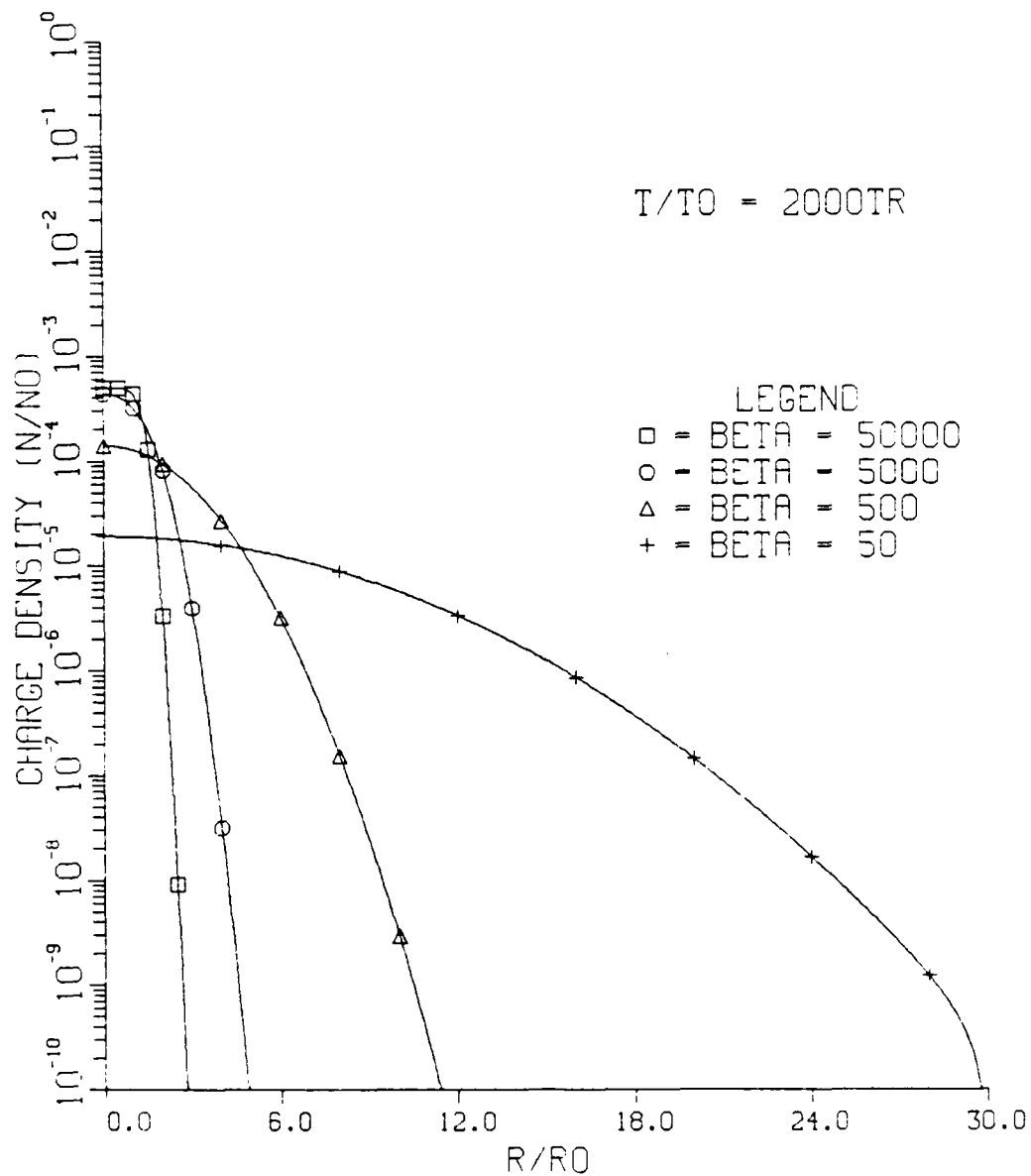


FIGURE 3.2

length of the streamer (or the distance between the electrodes in Figure 2.1 for this case). Additionally, m_e and ν_e are the electron mass and the electron collision frequency, respectively.

For the decaying streamer, the radius, and therefore the area, is changing but the length is constant. Since all the other factors within the brackets of Equation (3.2) are also constant, 'G' can then be expressed as,

$$G = \frac{e^2}{\lambda m_e \nu_e} \int_0^{\hat{r}} \hat{n} 2\pi \hat{r} d\hat{r} \quad (3.3)$$

where gamma is now defined as the value of the integral in the above equation. Gamma has the units of reciprocal meters, and is determined in the program, "CHARGE" (Appendix A), by the subroutine, "CNDUCT." Gamma is then directly proportional to the conductance.

Figure 3.3 shows gamma plotted over time out to 100TR. Note that gamma drops in value by 90% in only about 10TR (1.6 microsec). After this time the value levels off to about 0.04 at 100TR and then beyond the range of Figure 3.3 the value drops very slowly to about 0.001 at 10,000TR (1.6 msec).

Figure 3.3 is for fully laminar flow. Introducing turbulence into the flow causes a very slight increase in gamma over all time for the complete streamer. Figure 3.4

GAMMA VS TIME
IN LAMINAR FLOW

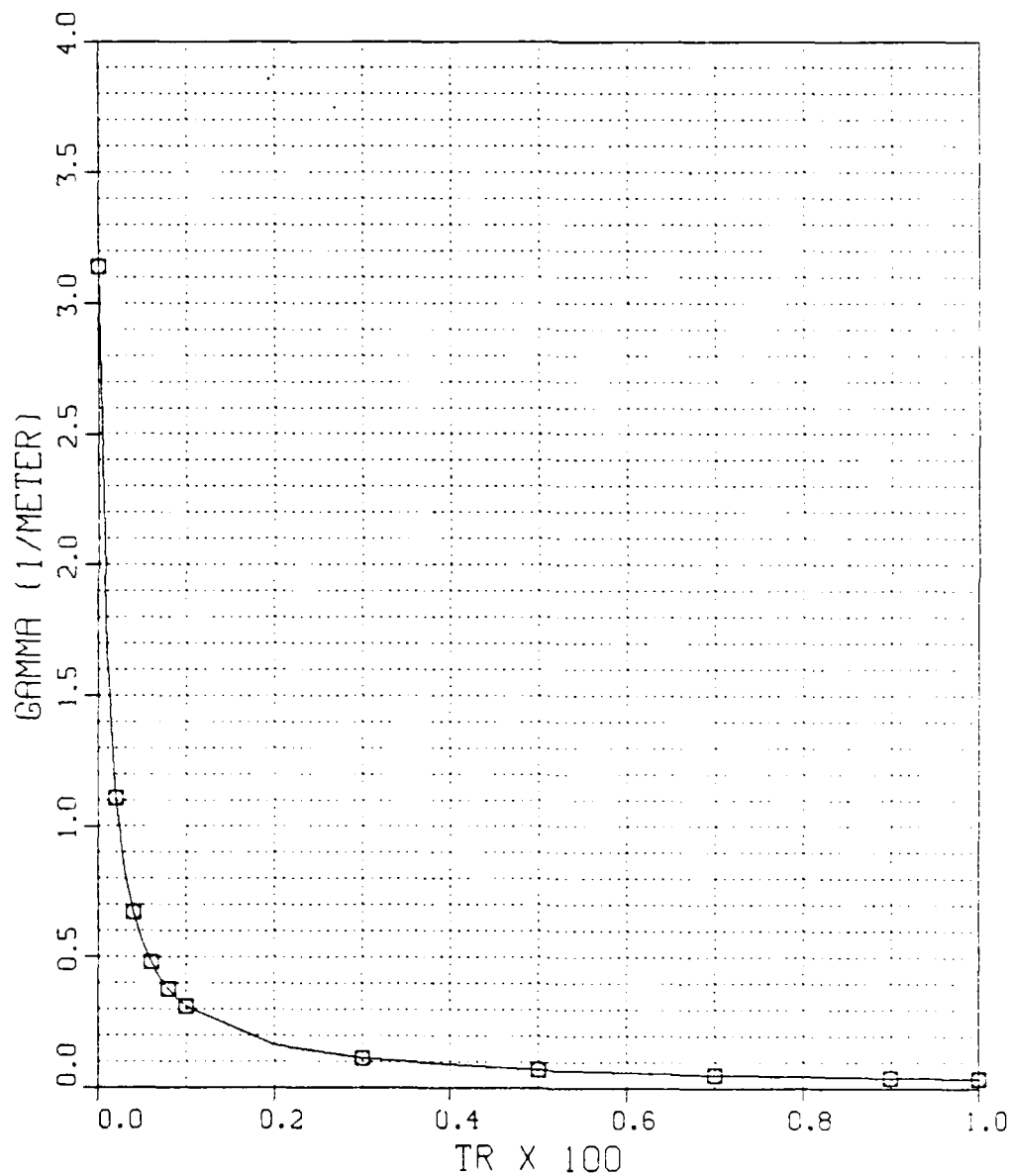


FIGURE 3.3

GAMMA VS BETA

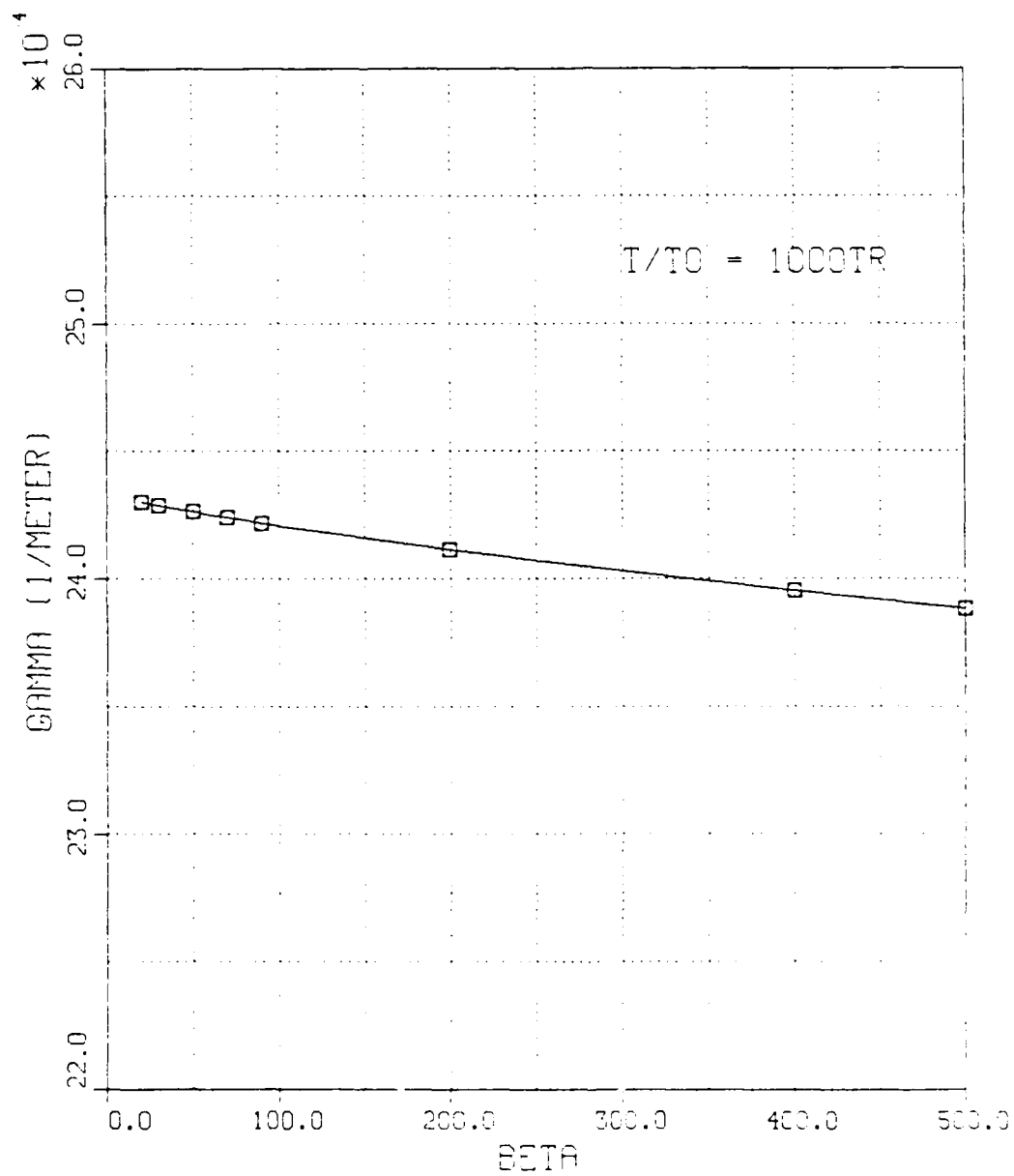


FIGURE 3.4

shows this effect at 1000TR. Figure 3.5 shows the value of gamma within the original streamer tube channel only. Here it is seen that for small beta (high turbulence) the conductance is lower than in the laminar flow condition.

Referring back to Figure 3.2, and with these conductance characteristics in mind, it seems rather apparent that one effect of the turbulence is to delay the possibility of a transition to arcing since the conductance is lower along the original channel. Another consideration is what happens to a follow-on streamer appearing after the charged particle density profile of the first streamer has died away for say, 2000TR as in Figure 3.2. In a laminar flow there would be a distinct path of least resistance along the original channel. However, in the turbulent flow, the profile is spread out over a much larger radius and then, this "follow-on streamer" essentially has no favored "route" for arcing.

Equation (2.30) showed that the charged particle density was the sole source of heating in this model. Figure 3.6 shows the result of solving Equation (2.30) in a fully laminar flow for an E/N of $1.635E-17 \text{ V-cm}^2$, at one atmosphere, and 300°K for an electric field strength of $4.0E4 \text{ V/m}$. Note that the temperature rise amounts to less than about 0.05% in 1000TR and then rises very slightly over time eventually peaking out at about 4000TR and then falling back slowly. This would seem to be a logical behavior for this case since the charged particle density that is heating the gas is also

GAMMA VS BETA
FOR STREAMER TUBE

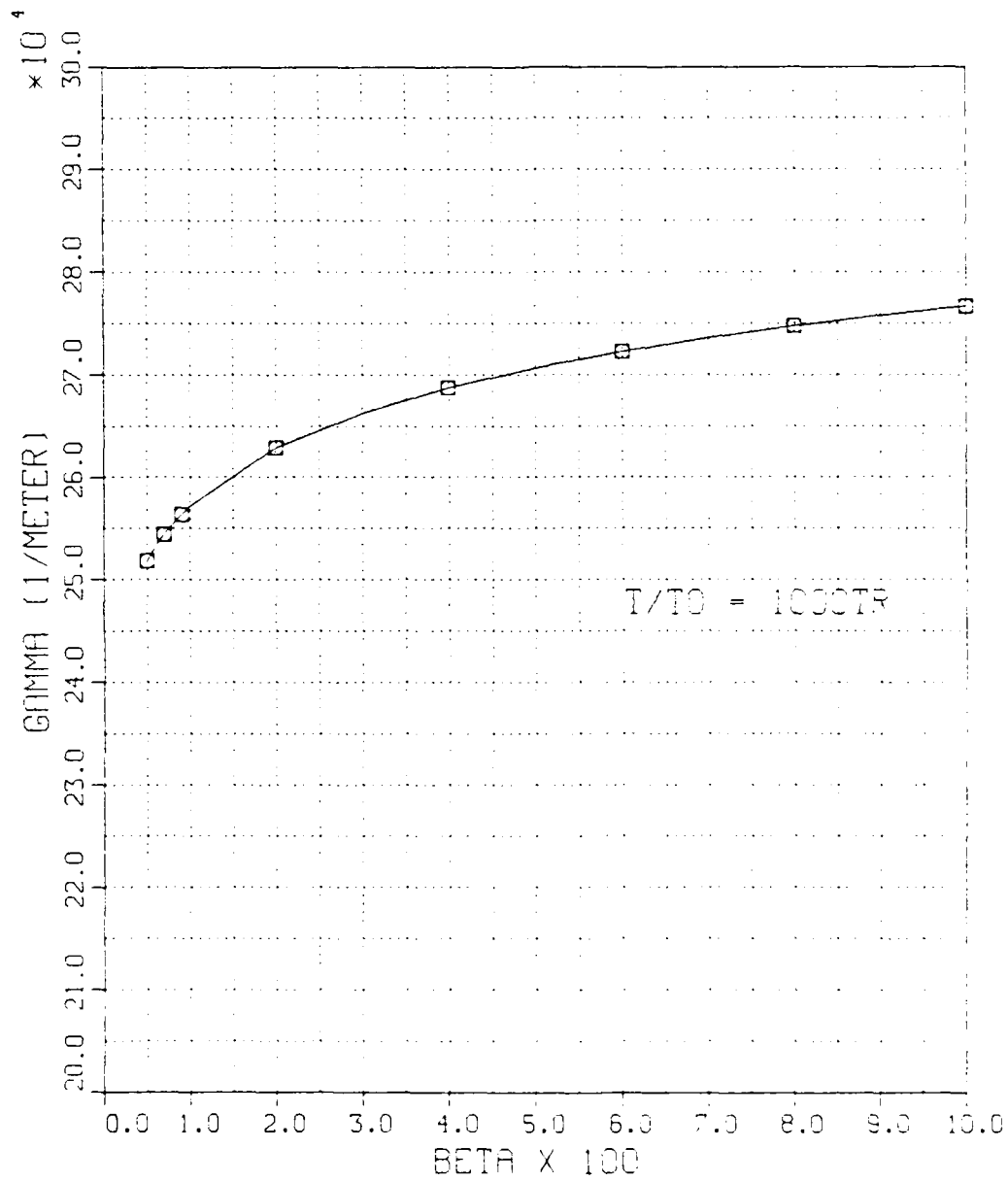


FIGURE 3.5

dying away. The question is then; what happens if one increases the electric field?

Figures 3.7 through 3.10 show the effects of increasing E_0 from $1.0E6$ V/m (a typical value of interest for lasers) to $8.0E6$ V/m. Note that β_A changes for each of these cases. This is due to the fact that the electron drift velocity is a function of E/N , which is plotted in Figure 2.2. Since the drift velocity changes, the electron mobility changes which, in turn, produces a new conductivity value for each different electric field strength case. Recalling Equations (2.20) and (2.23), one can see that each case has a different characteristic time and a different β_A . For increasing E_0 , τ_A gets smaller while β_A gets larger.

The main difficulty with this is that the time step for the energy equation solution must be adjusted to ensure that the continuity equation is "feeding" the charged particle density values into the energy equation at the correct rate. For the continuity equation, the non-dimensionalized time step is 0.1 ($\tau_R/10$ in real time). Therefore, the true time for one time step (one "DT" in the program) is simply $DT \times \tau_R$. Similarly, the true time for the energy equation is $DTA \times \tau_A$. It follows then that the value needed for DTA is simply $(DT \times \tau_R) / \tau_A$.

Returning to Figures 3.7 through 3.10, it can be clearly seen that increasing E_0 increases the temperature rise, as would be expected. The effects of longer times is the same as the case for Figure 3.6 but requires much longer computing

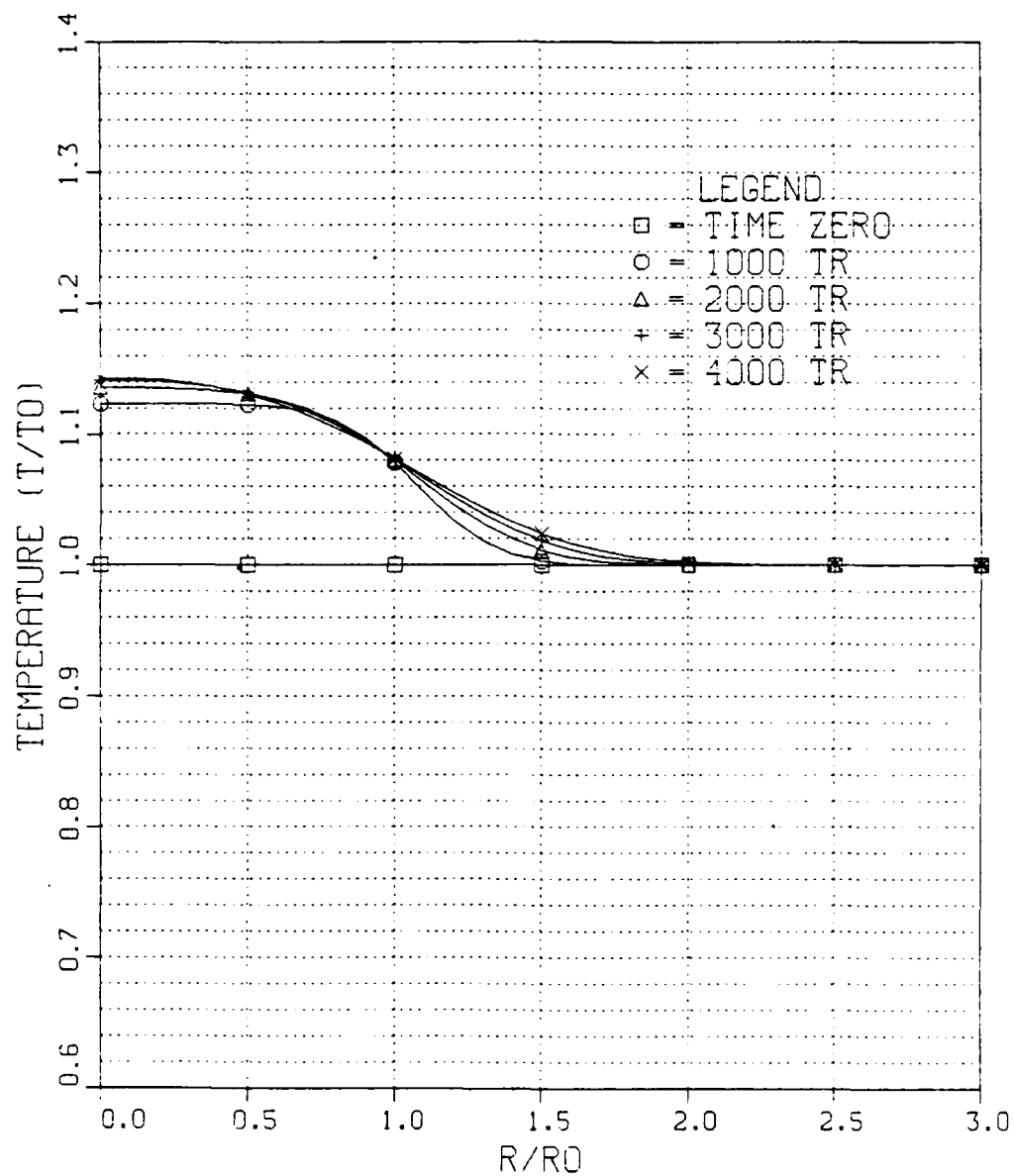
TEMPERATURE PROFILEFOR $E = 1.0E6$ V/M

FIGURE 3.7

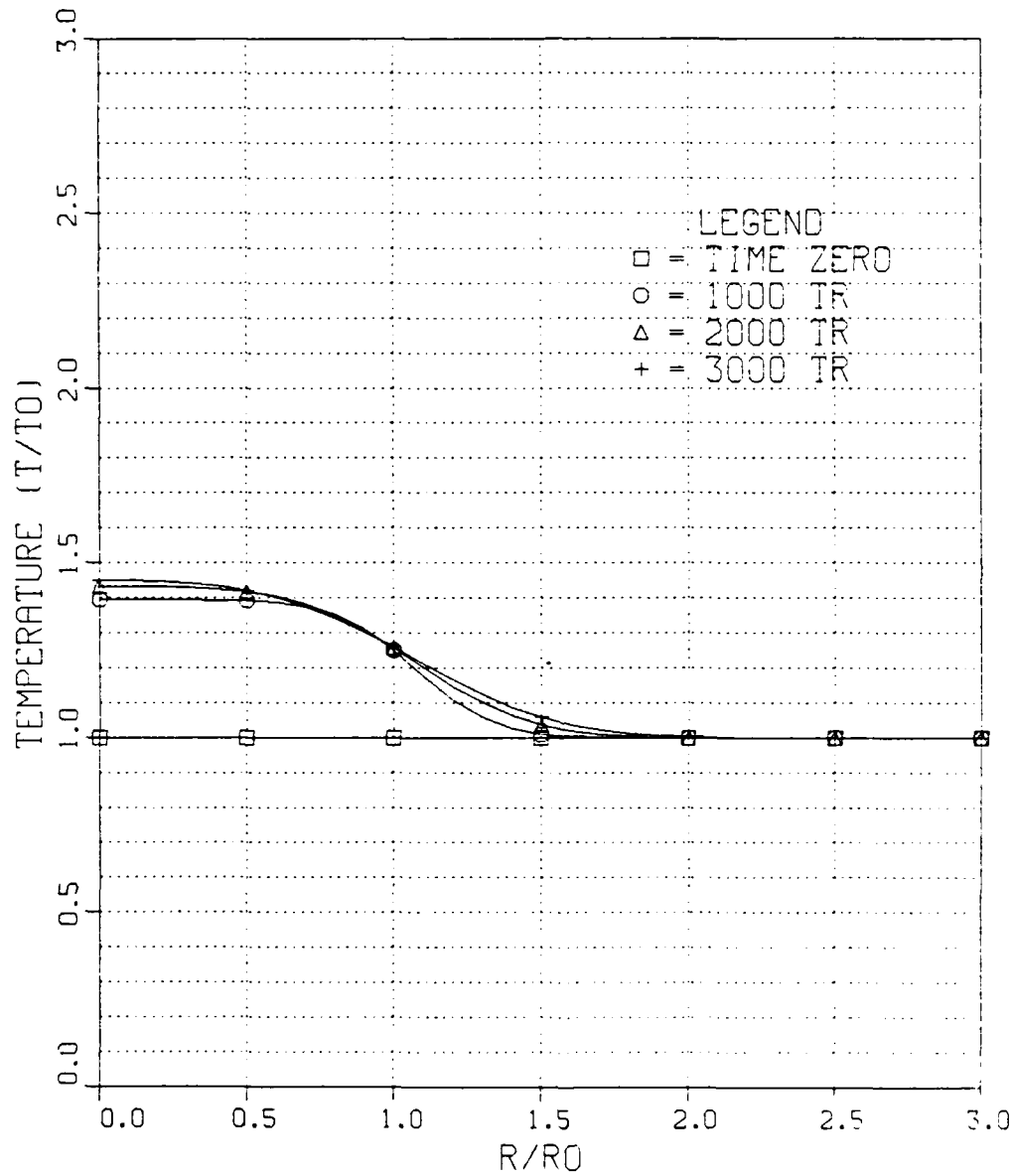
TEMPERATURE PROFILEFOR $E = 2.0 \times 10^6$ V/M

FIGURE 3.8

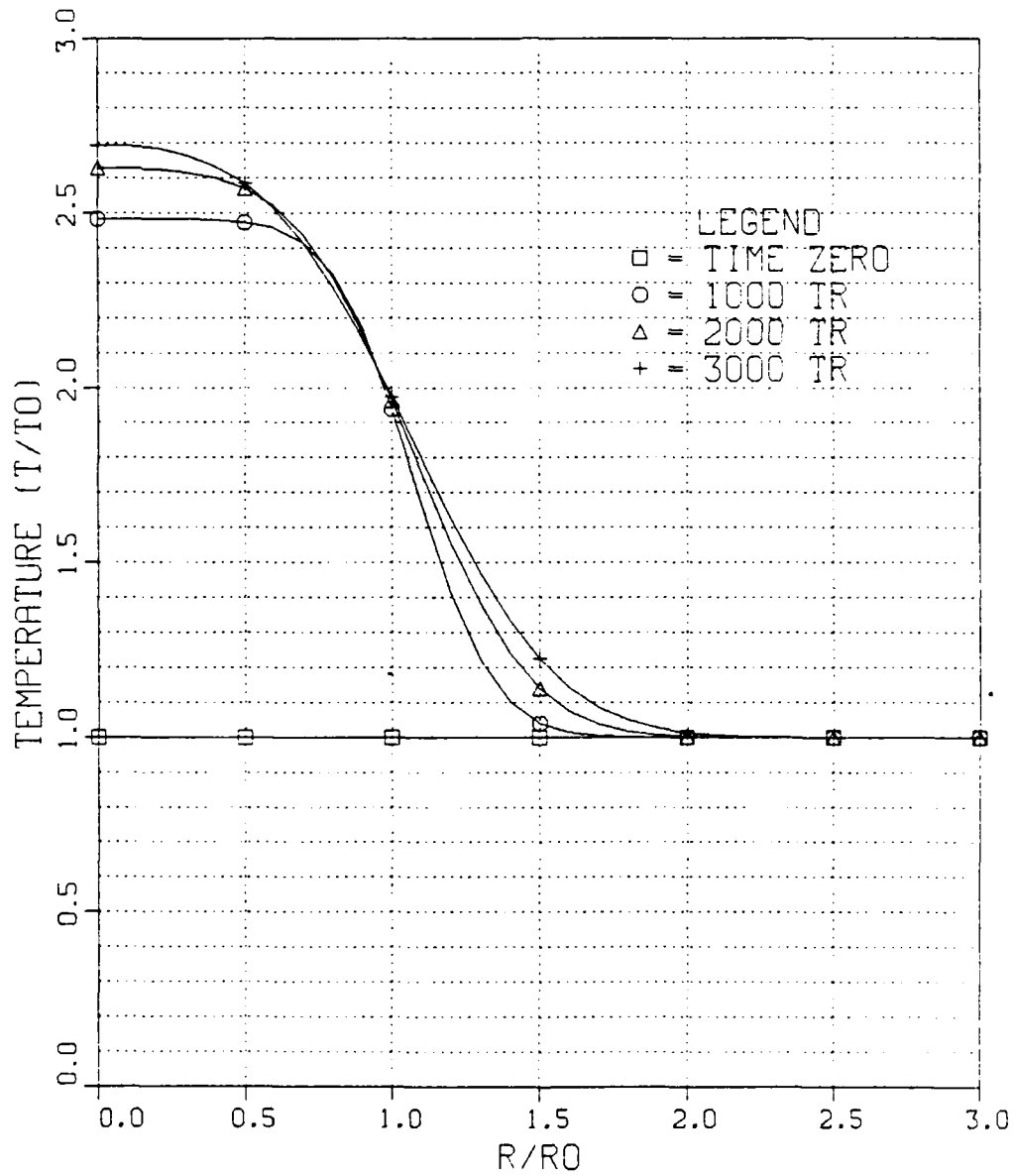
TEMPERATURE PROFILEFOR $E = 4.0E6$ V/M

FIGURE 3.9

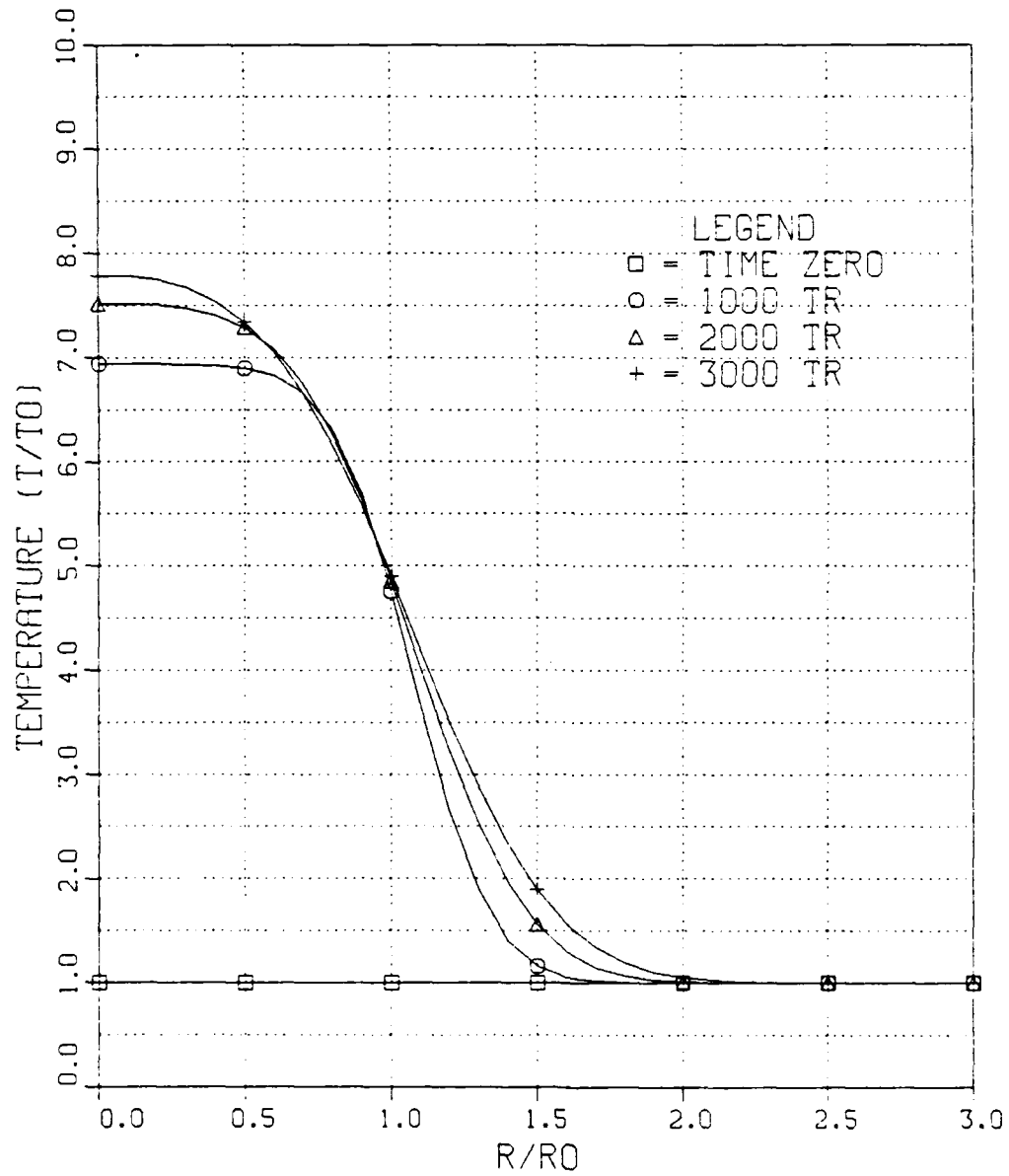
TEMPERATURE PROFILEFOR $E = 8.0E6$ V/M

FIGURE 3.10

times to reach the peak and to begin falling back. The effect of turbulence on the cases of interest, say $4.0E4$ V/m to $1.0E6$ V/m, is to essentially eliminate the temperature rise.

One remaining question for this non-ionized case is what effect would increasing n_0 have? Figure 3.11 shows that at $E_0 = 1.0E6$ V/m and n_0 increased by a factor of 10 to $3.125E19/m^3$ produces a more squared off profile than that depicted in Figure 3.7 suggesting that the temperature dies rapidly outside of the immediate influence of the streamer. Figure 3.12 shows the effect of another 10-fold increase in N . Here the resulting temperature rise drops off at an even steeper rate at 2000TR than for Figures 3.7 and 3.11. Recalling that $\tau_R = 1/\alpha_2 n_0$, it is clear that increasing n_0 decreases the characteristic recombination time significantly which, in turn, lowers \hat{n} such that there is a noticeable reduction in the temperature profile outside of this immediate streamer influence.

B. IONIZED ENVIRONMENT CASE

In this section the effects of a glow discharge in an environment where a steady glow exists is considered. For this situation, Equation (3.4) is the applicable non-dimensional form of the governing continuity equation.

$$\frac{\partial \hat{n}}{\partial \hat{t}} - \frac{1}{\beta \hat{r}} \frac{\partial}{\partial \hat{r}} \left(\hat{r} \frac{\partial \hat{n}}{\partial \hat{r}} \right) = \hat{n} - \hat{n}^2 - \alpha \hat{n}^3 \quad (3.4)$$

TEMPERATURE PROFILE

FOR $N_0 = 3.125 \times 10^{19} \text{ M}$

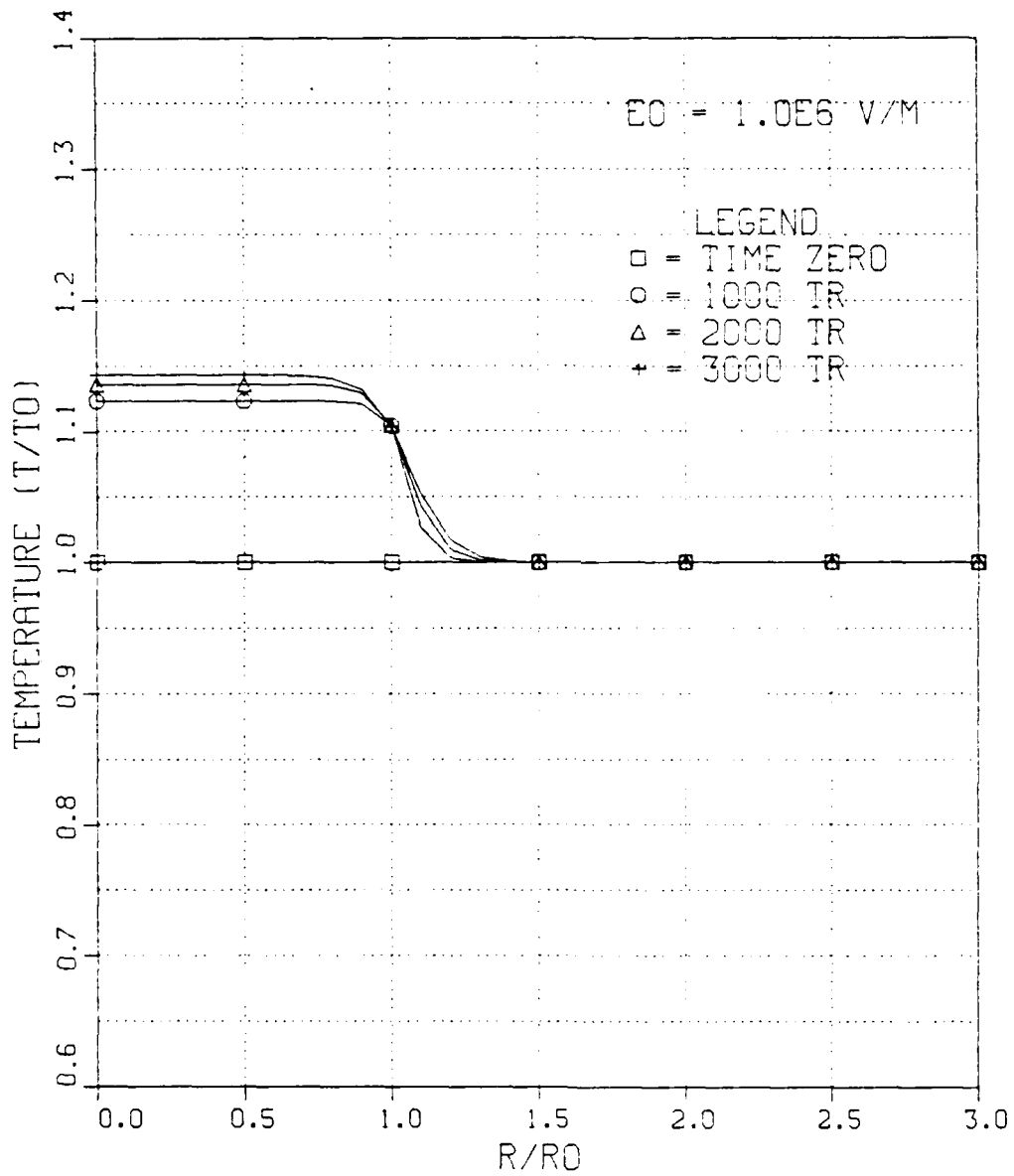


FIGURE 3.11

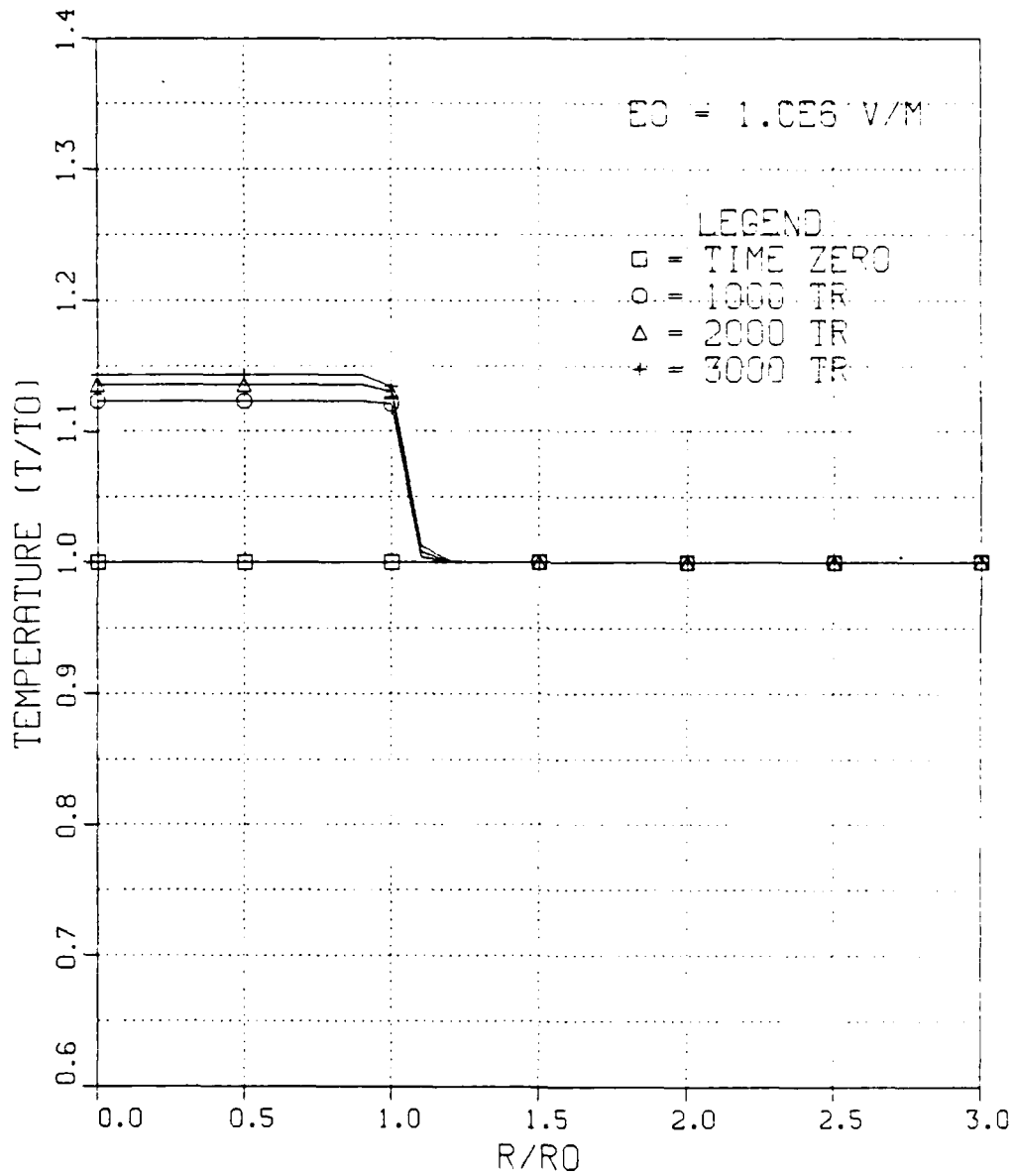
TEMPERATURE PROFILEFOR NO = 3.125E20 M

FIGURE 3.12

The temperature effects are then determined by Equation (2.30) where \hat{n} is obtained by solving Equation (3.4). The first question in this case might be; what effect does turbulence have on the temperature profile due to this steady glow discharge? At sub-atmospheric pressure, it is known that the charged particle density profile takes on a Bessel function distribution [Ref. 9]. Therefore, to investigate this situation, Equation (2.30) can be solved independently from Equation (3.4) by calling up the subroutine "DENSTY" in the program and sending it a constant, for all time, value for \hat{n} . The Bessel function serves as the initial condition profile for the value of \hat{n} . This distribution, labeled "N1" in the program, allows \hat{n} to go to zero at $r = 4.8$. Figure 3.13 shows the results of such a case for strictly laminar flow. The values of the controlling parameters for Figures 3.13 through 3.16 are: $n_0 = 3.125E18 \text{ m}^{-3}$, $\alpha_2 = 2.0E-12 \text{ m}^3/\text{sec}$ and $E_0 = 1.0E6 \text{ V/m}$. It is clearly evident that the temperature for such a laminar case would rise to approximately 5400°K (recall that $T/T_0 = 1$ is equivalent to 300°K) in only about 1000TR. Since molecular nitrogen (N_2) begins to dissociate at about 4000°K , the situation depicted in Figure 3.13 is undesirable. However, introducing turbulence into the flow tends to significantly reduce this temperature distribution. Figure 3.14 shows that a moderate degree of turbulence can be selected which, essentially, holds the temperature profile near the laminar profile without

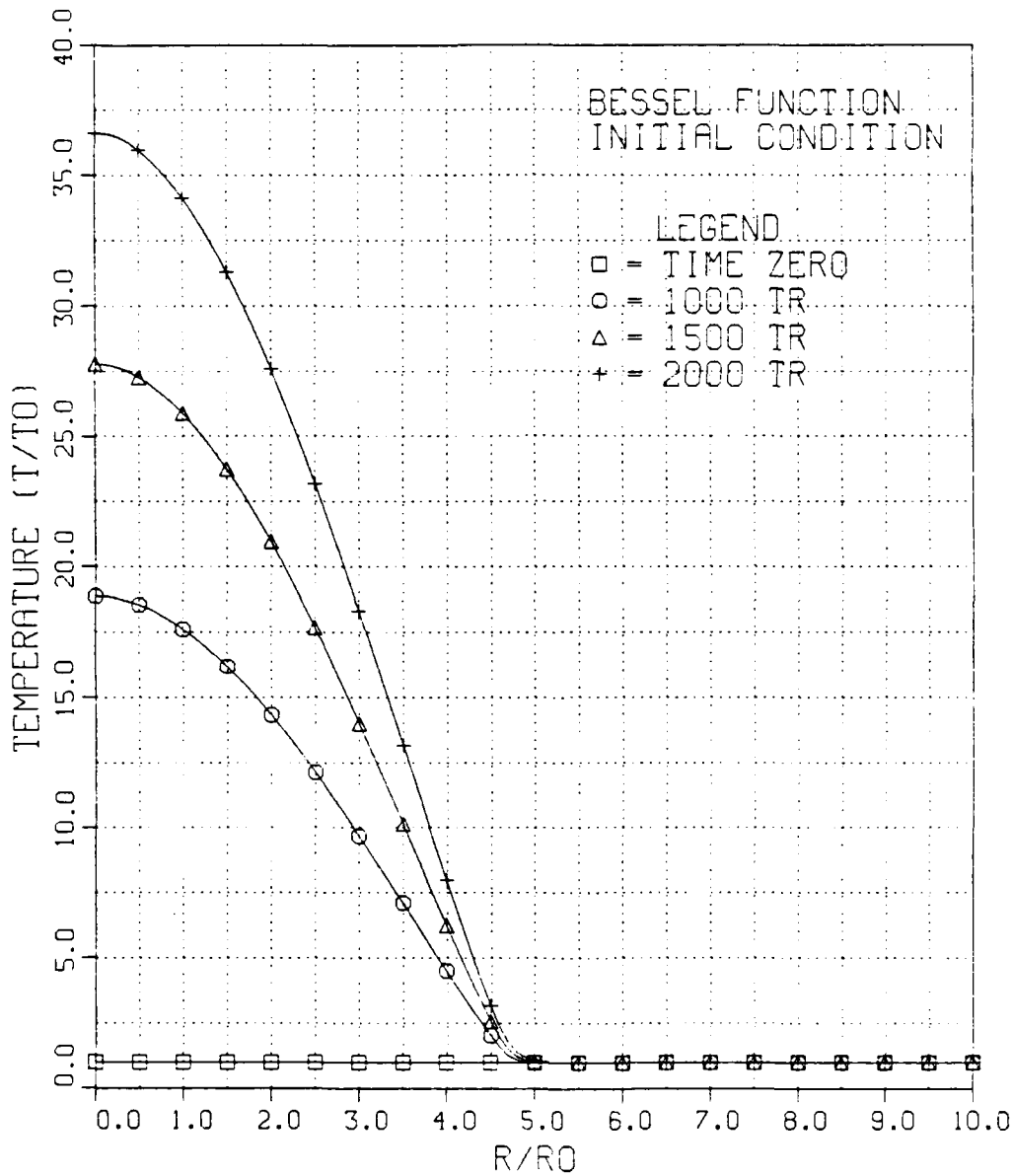
TEMPERATURE PROFILEFOR BARMIN = 800

FIGURE 3.13

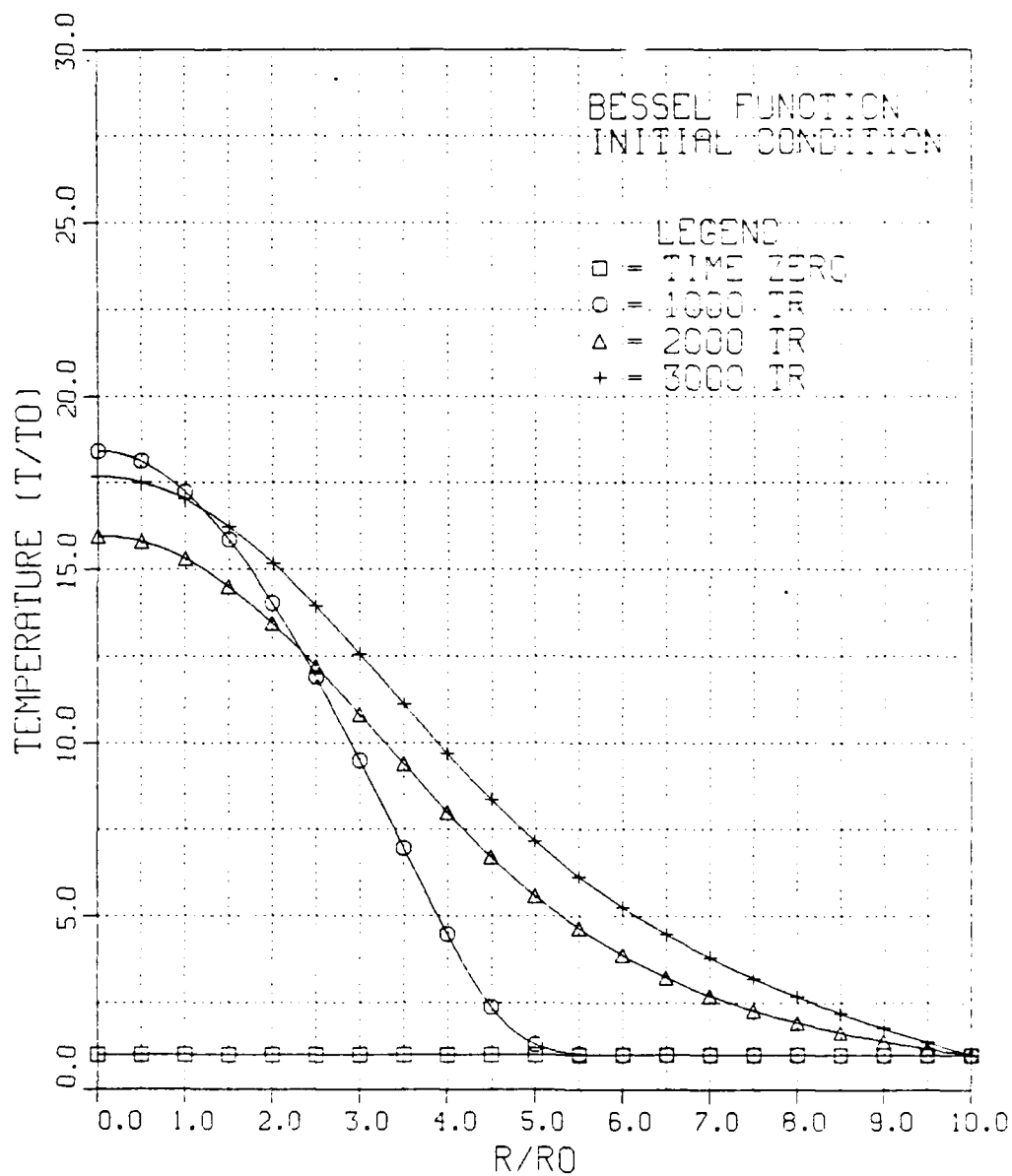
TEMPERATURE PROFILEFOR BAFIN = 3

FIGURE 3.14

TEMPERATURE PROFILE

FOR B A M I N = 1

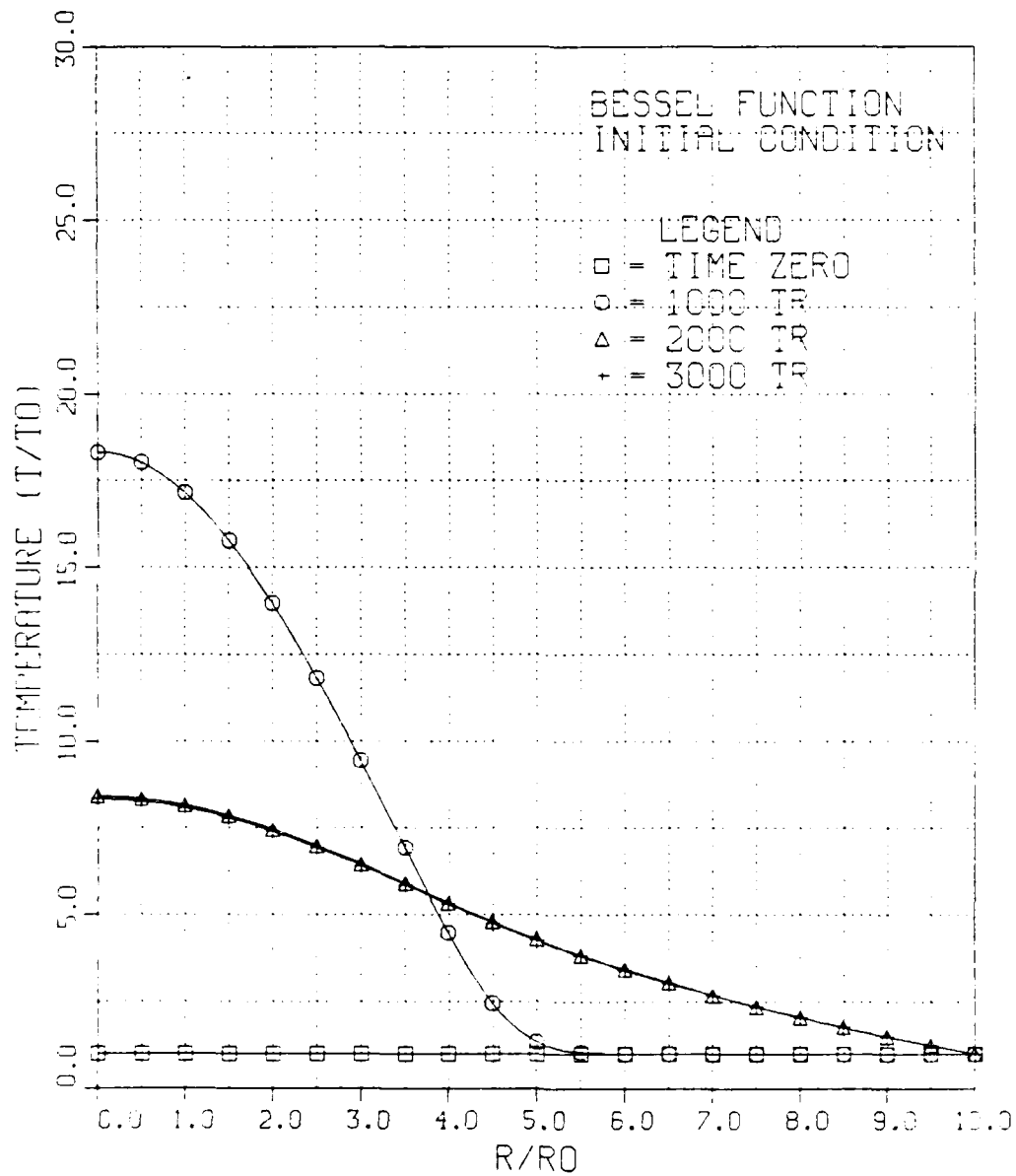


FIGURE 3.15

TEMPERATURE PROFILE

FOR BARMIN = 0.4

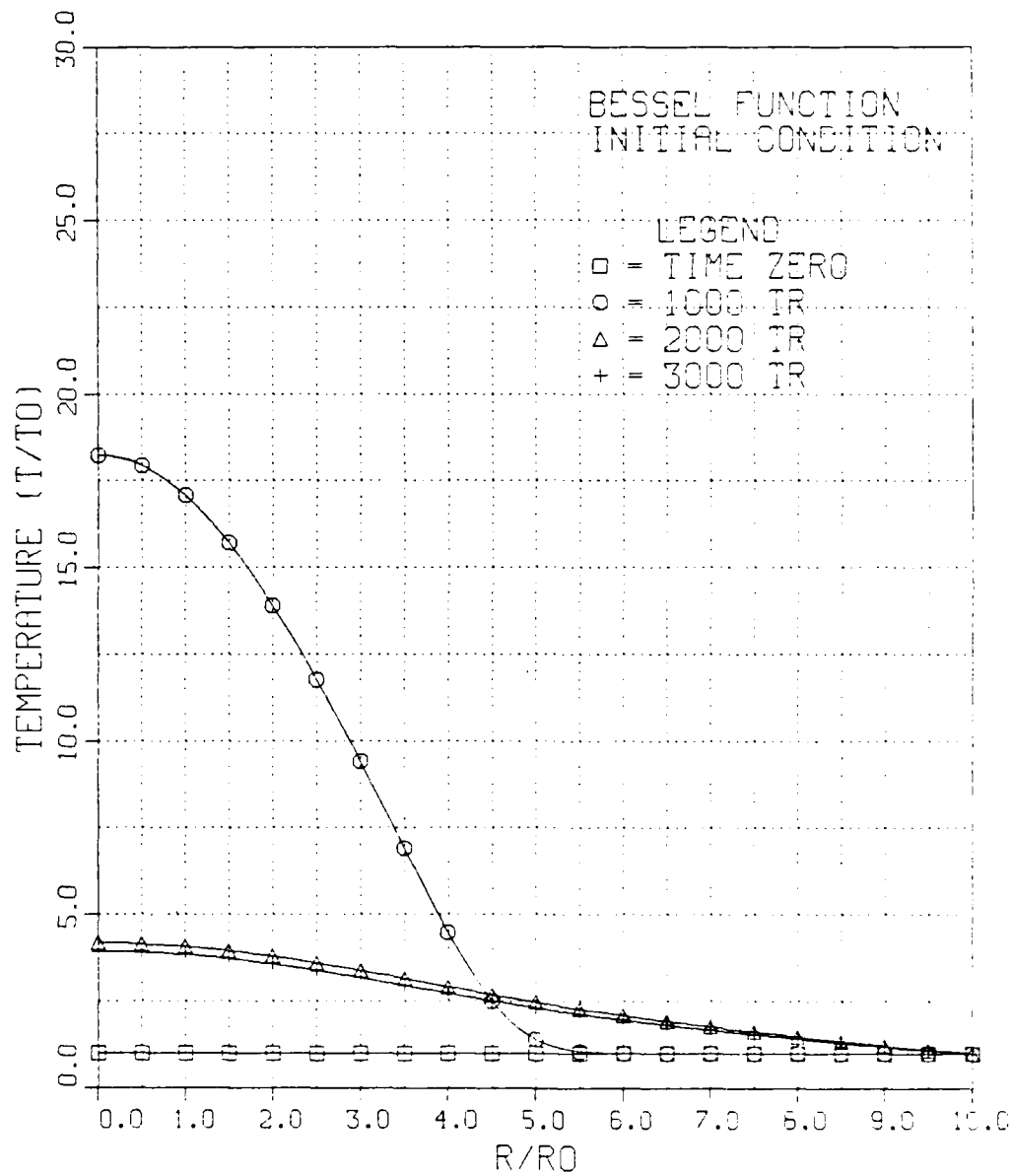


FIGURE 3.16

going unstable as in Figure 3.13. Figures 3.15 and 3.16 show the effects of increasing the turbulence level still further. Note that in Figure 3.15, the temperature profile is nearly "frozen out" at about 2400°K, while Figure 3.16 is holding steady at around 1200°K.

This asymptotic behavior of the temperature rise in reaching this stable profile appears to be related to the characteristic time associated with Equation (2.30). Observe that for all three figures (3.14, 3.15 and 3.16) the temperature rise stabilizes between about 2000TR and 3000TR. This effect will continue to be evident in the remaining cases to be discussed. The parameters for the case presently being considered are such that the true time of 2500TR is 0.4 msec. This is approximately 4.5 times the characteristic time step in seconds for the energy equation, which is consistent with the concept of a rise time in an asymptotic system.

The final case to be discussed here is perhaps the most interesting. This will be the case where there is a steady level of ionization in the gas and a perturbation of the electric field is introduced to model the effects of the streamer. For the steady state situation at the centerline, $\frac{\partial n}{\partial t} = 0$, so one can write Equation (3.5).

$$-\frac{D_a}{r} \frac{\partial}{\partial r} \left(r \frac{\partial n}{\partial r} \right)_{\zeta} = 0 = \nu_i n_{\zeta} - \alpha_2 n_{\zeta}^2 - \alpha_3 n_{\zeta}^3 \quad (3.5)$$

Neglecting the three-body recombination term (α_3 is on the order of $1.0E-34 \text{ m}^6/\text{sec}$), and noting that $\frac{\partial n}{\partial r}$ on the centerline

is also zero, the ionization term is then equal to $\alpha_2 n_e$. Since Figure 2.2 gives v_i/N , the charged particle density for the steady state condition can be obtained by,

$$n_e \approx \frac{v_i}{\alpha_2} = \left(\frac{v_i}{N}\right) \left(\frac{N}{\alpha_2}\right) \quad (3.6)$$

where N is given by Equation (2.28). Figure 3.17 shows this steady state charged particle distribution where, for this model, the glow discharge is contained in a region of a radius equal to $10 r_0$. At r_0 , the boundary condition is set such that \hat{n} is zero at the "wall." The left hand boundary condition assumes that the slope of the charged particle density is zero. See Appendix A for details concerning how the program meets these boundary conditions. Note that in Figure 3.17, the steady state condition is reached in less than 100TR, and is constant at the longer times. The first vertical line, at $r/r_0 = 1.0$, is the initial condition distribution which assumes $\hat{n} = 1.0$ out to $\hat{r} = 1.0$ and zero beyond this point.

The steady state solution for Equation (2.30) is given in Equation (3.7).

$$\hat{T} = -(\beta_A \hat{n}) \frac{\hat{r}^2}{4} + \beta_A \frac{\hat{n} b^2}{4} + \hat{T}_0 \quad (3.7)$$

The boundary conditions are $\hat{T} = T_0$ at $\hat{r} = b$ and $\frac{\partial \hat{T}}{\partial \hat{r}} = 0$ at $\hat{r} = 0$. Figure 3.18 shows this result for $E_0 = 1.47E5$ V/m. For this case $\beta_A = 0.2219$, and so at the centerline $\hat{r} = 0$

CHARGED PARTICLE DENSITY PROFILE
WITH IONIZATION TERM

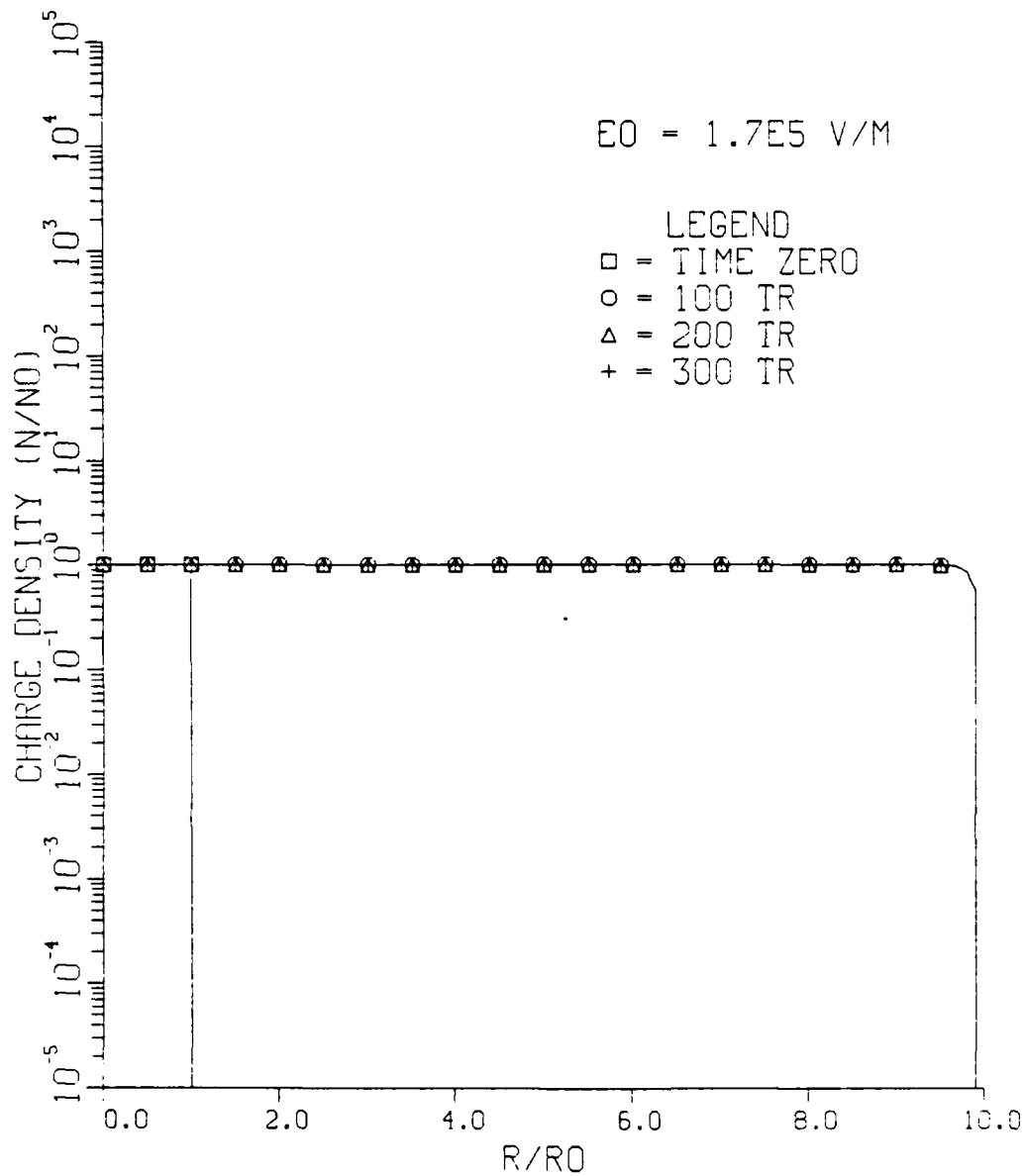


FIGURE 3.17

TEMPERATURE PROFILE
IN TURBULENT FLOW

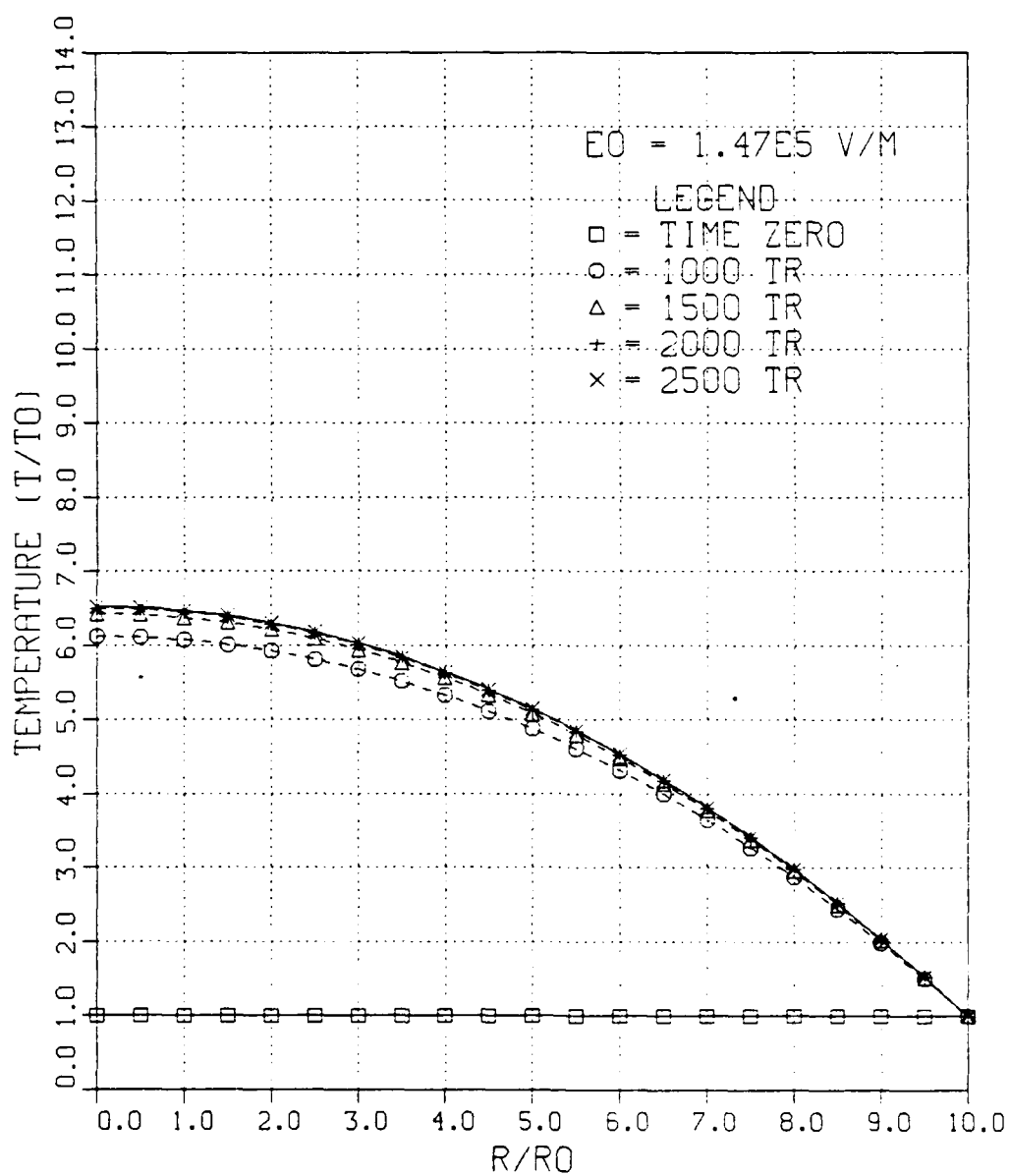


FIGURE 3.18

and substituting in the appropriate values into Equation (3.7) one obtains $\hat{T} = 6.548$ which is confirmed at $\hat{r} = 0$ in Figure 3.18. Note that this steady state condition is reached at approximately 2500TR which is about the same time period required for stabilization from the previous case for the Bessel function initial condition profile (Figures 3.14, 3.15 and 3.16) and for the case showing the temperature profile of a lone streamer in a non-ionized environment (Figures 3.6 through 3.12).

Figures 3.19 through 3.28 show the results of introducing the electric field perturbation into the model. Each plot shows the situation of the streamer appearing in a steady state turbulent environment and lasting for increasing periods of time beginning at 5 recombination times and being incremented by 5TR up to a final value of 50TR. In real time, this would be equivalent to 0.6 msec to 6.0 msec. For these plots, $E_0 = 1.47E5$ V/m which produces an E/N of $6.0E-17$ V-cm². This case was chosen for example purposes since the steady state temperature profile is convenient at a centerline value of $T/T_0 = 6.5$ and the rise due to the perturbation reaches a maximum of about 13.75 (4125°K) at 50TR. Each figure shows five curves, 3 are solid and 2 are dashed. The solid lines represent the initial temperature distribution ($\hat{T} = 1.0$), the steady state profile, and then, the profile of the streamer at the end of its stay time. The dashed lines are the decaying, or transient, profiles produced after the appearance of

TEMPERATURE PROFILE
WITH STREAMER ON 5 TR

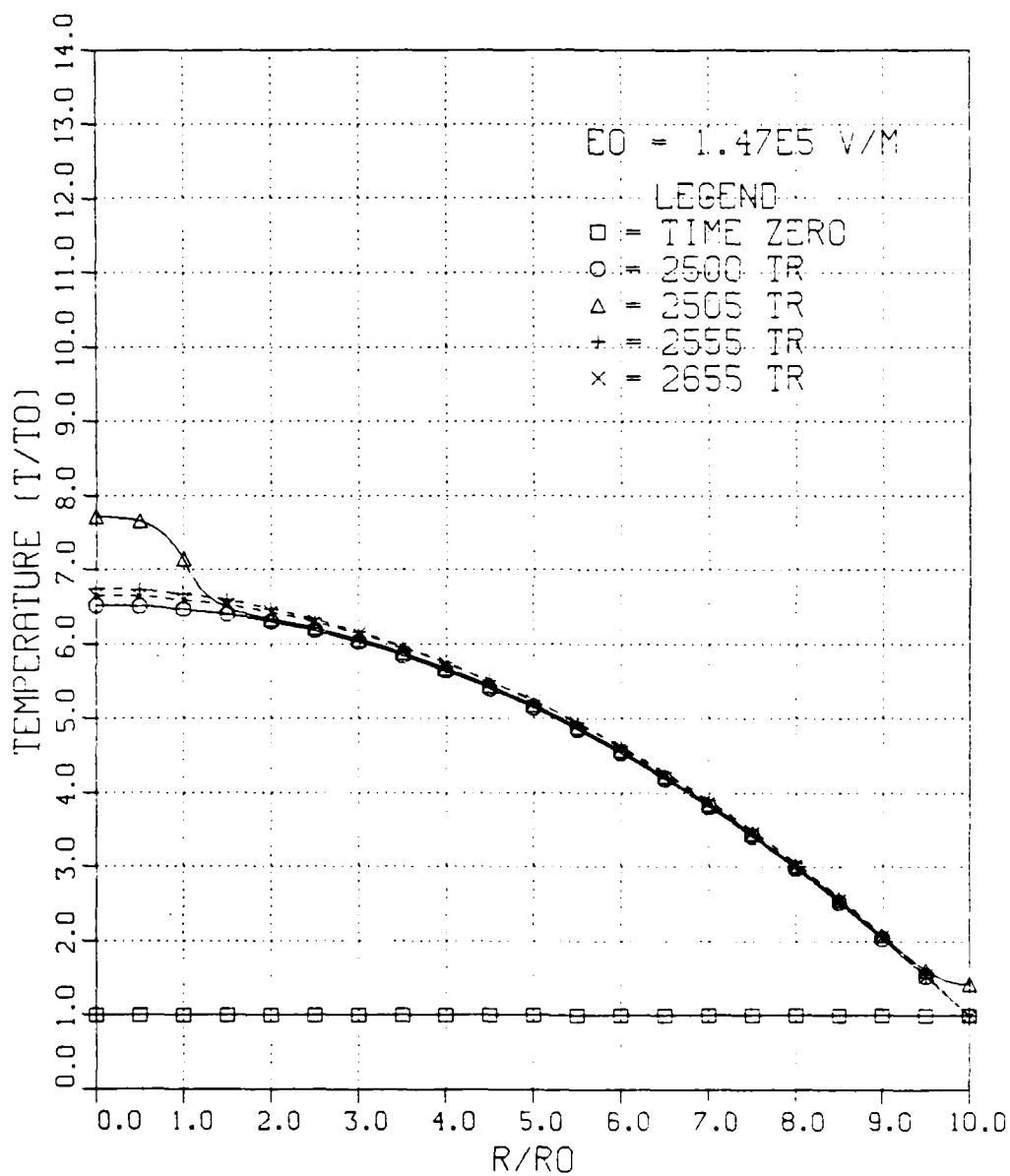


FIGURE 3.19

TEMPERATURE PROFILE
WITH STREAMER ON 10 TR

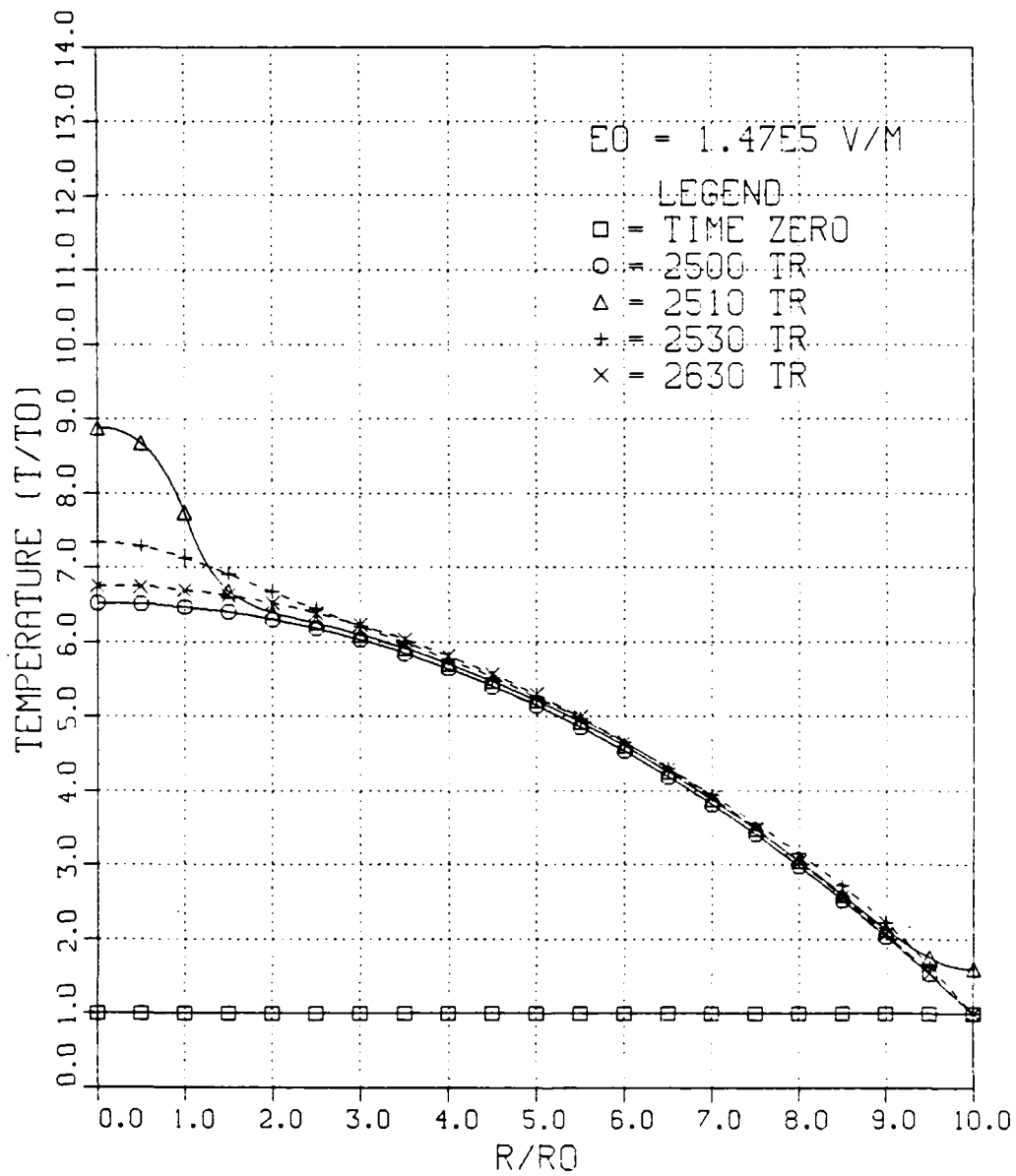


FIGURE 3.20

TEMPERATURE PROFILE
WITH STREAMER ON 15 TR

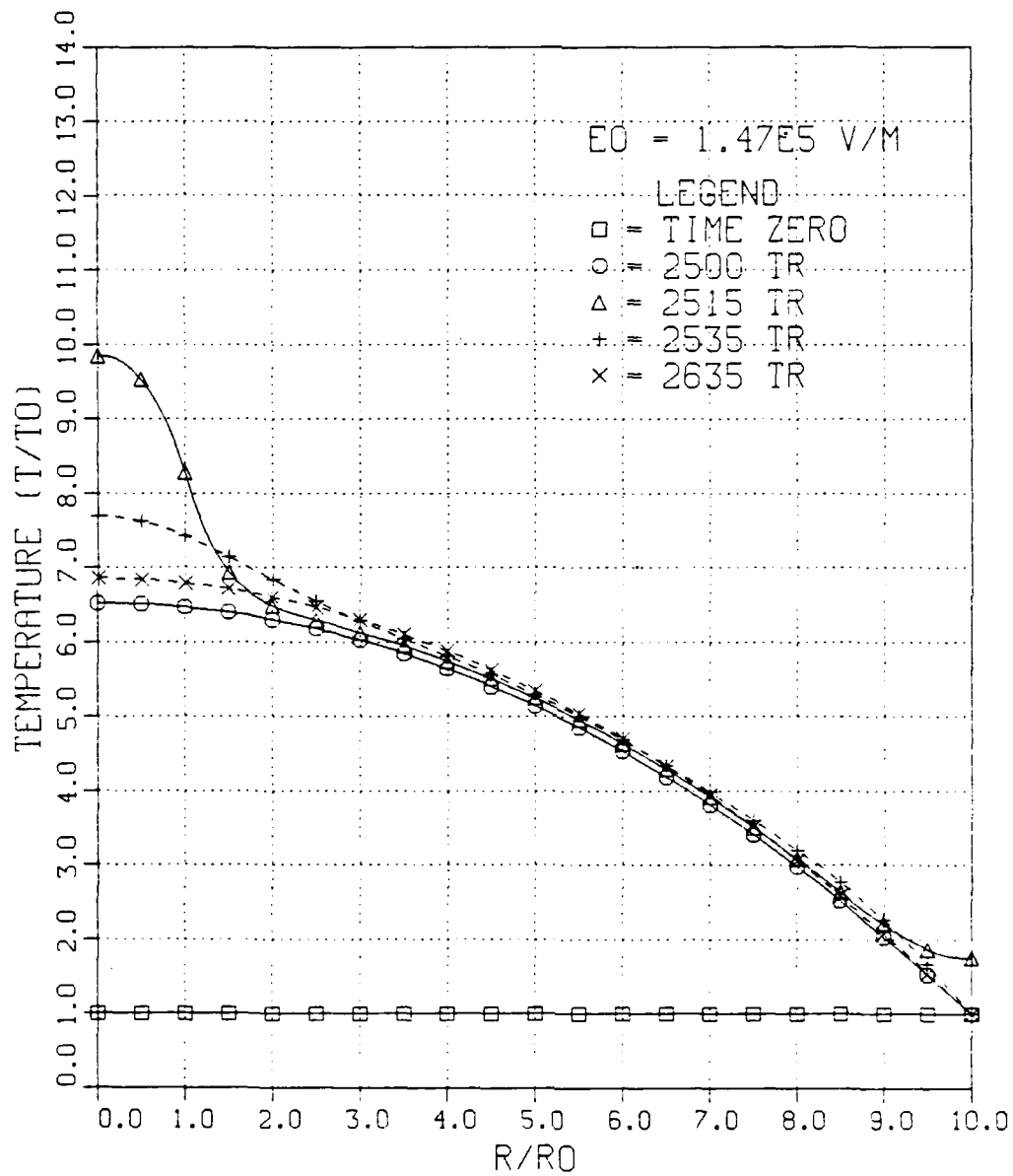


FIGURE 3.21

TEMPERATURE PROFILE
WITH STREAMER ON 20 TR

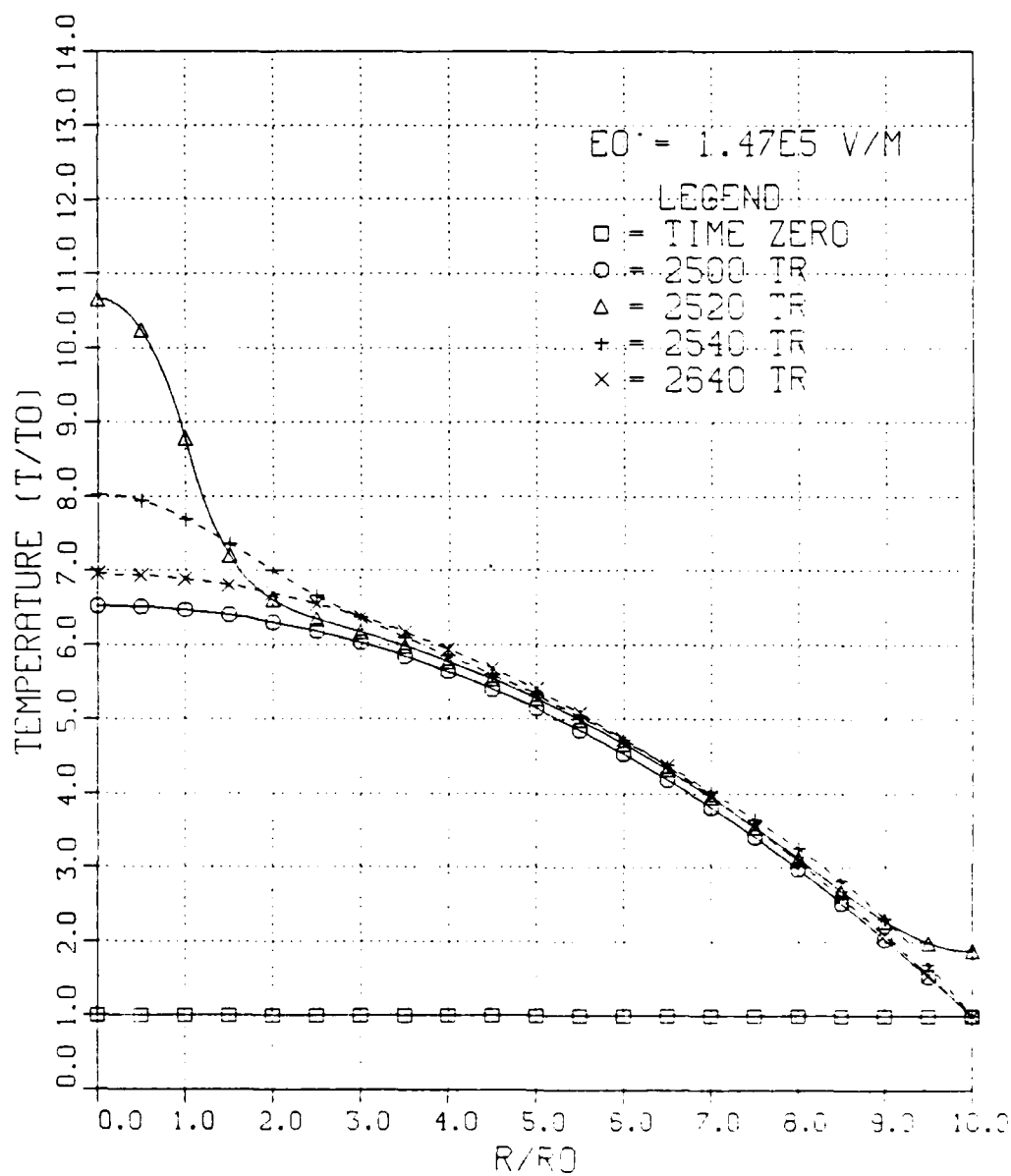


FIGURE 3.22

TEMPERATURE PROFILE
WITH STREAMER ON 25 TR

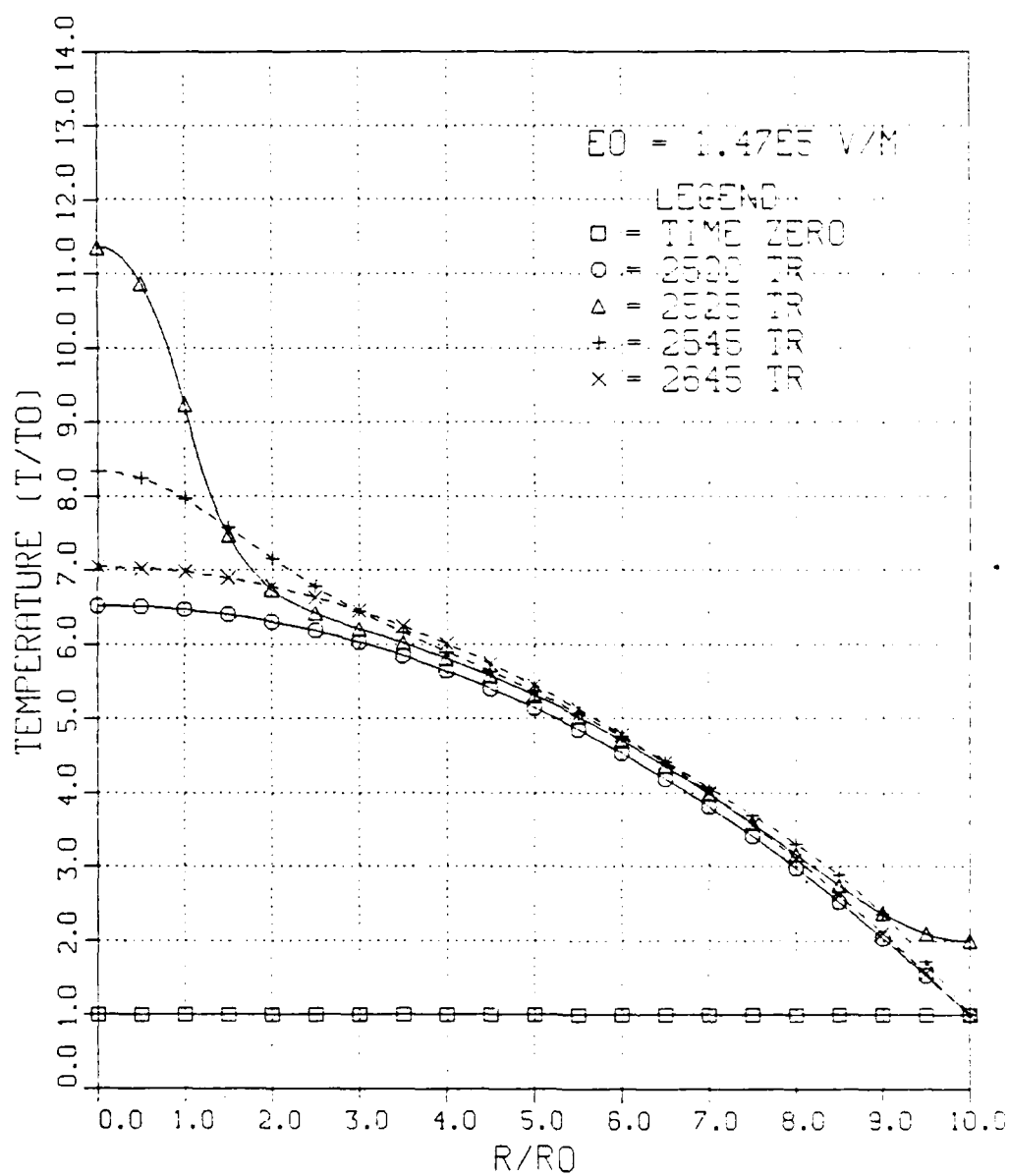


FIGURE 3.23

TEMPERATURE PROFILE
WITH STREAMER ON 30 TR

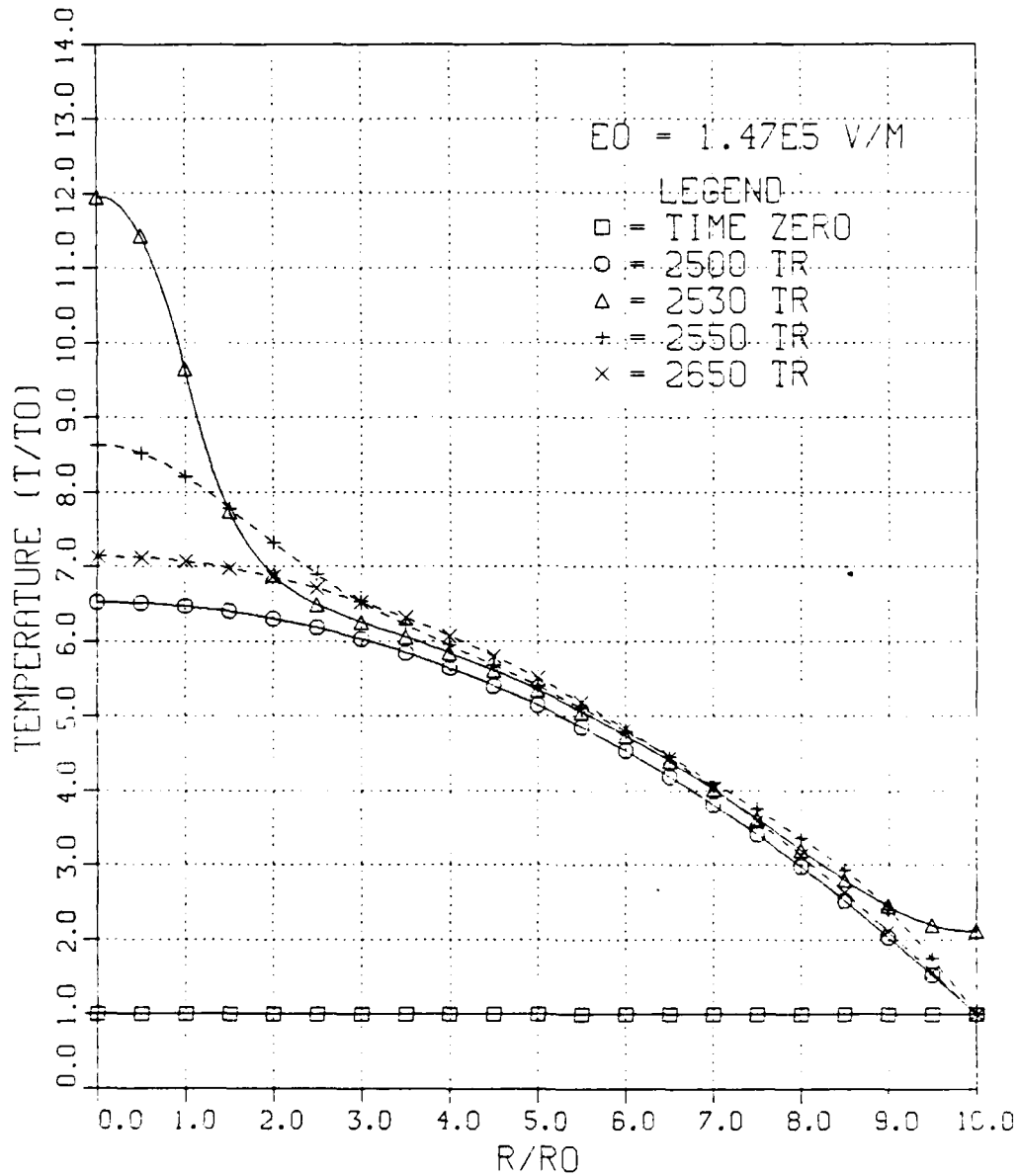


FIGURE 3.24

TEMPERATURE PROFILE
WITH STREAMER ON 35 TR

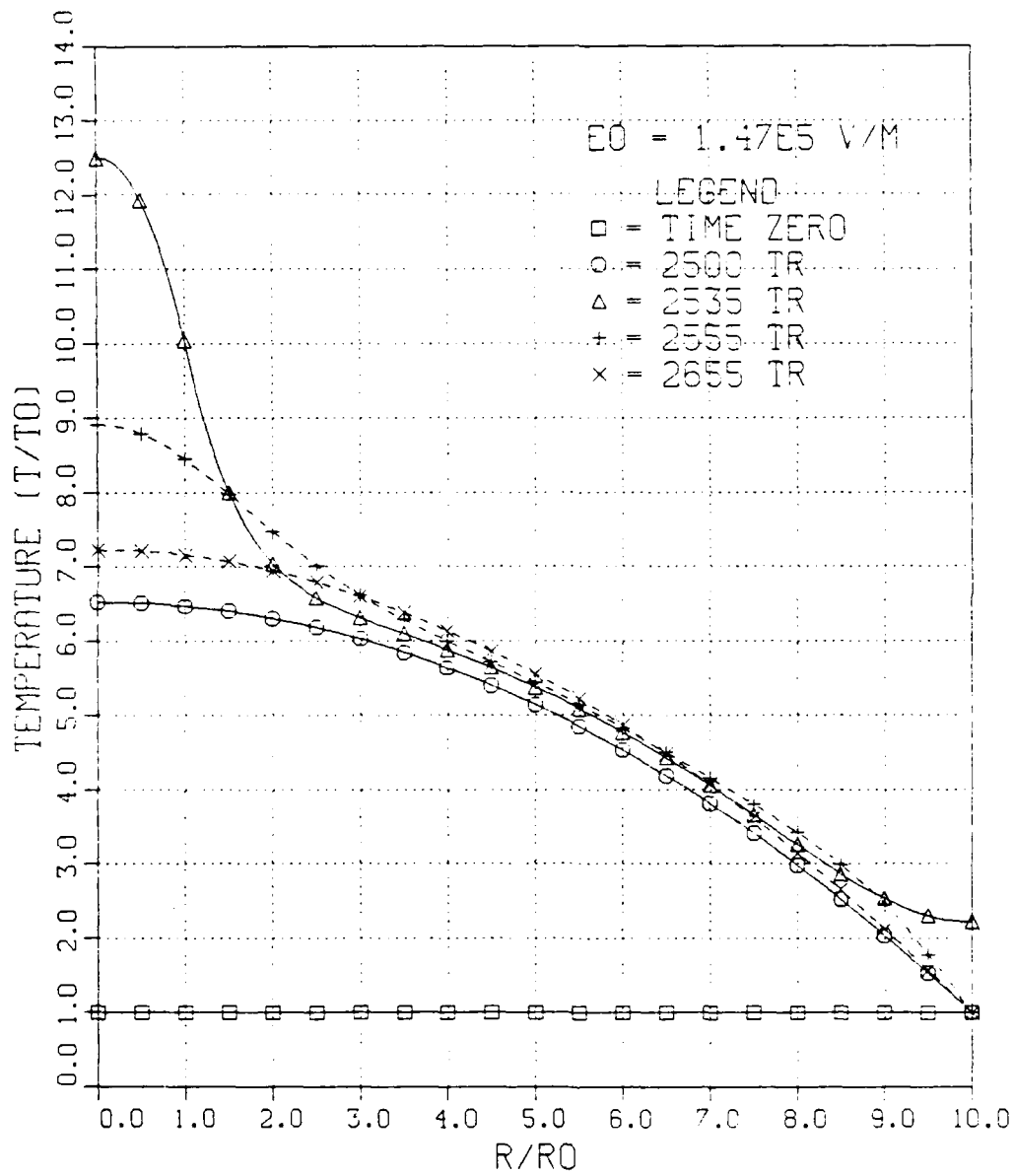


FIGURE 3.25

TEMPERATURE PROFILE
WITH STREAMER ON 40 TR

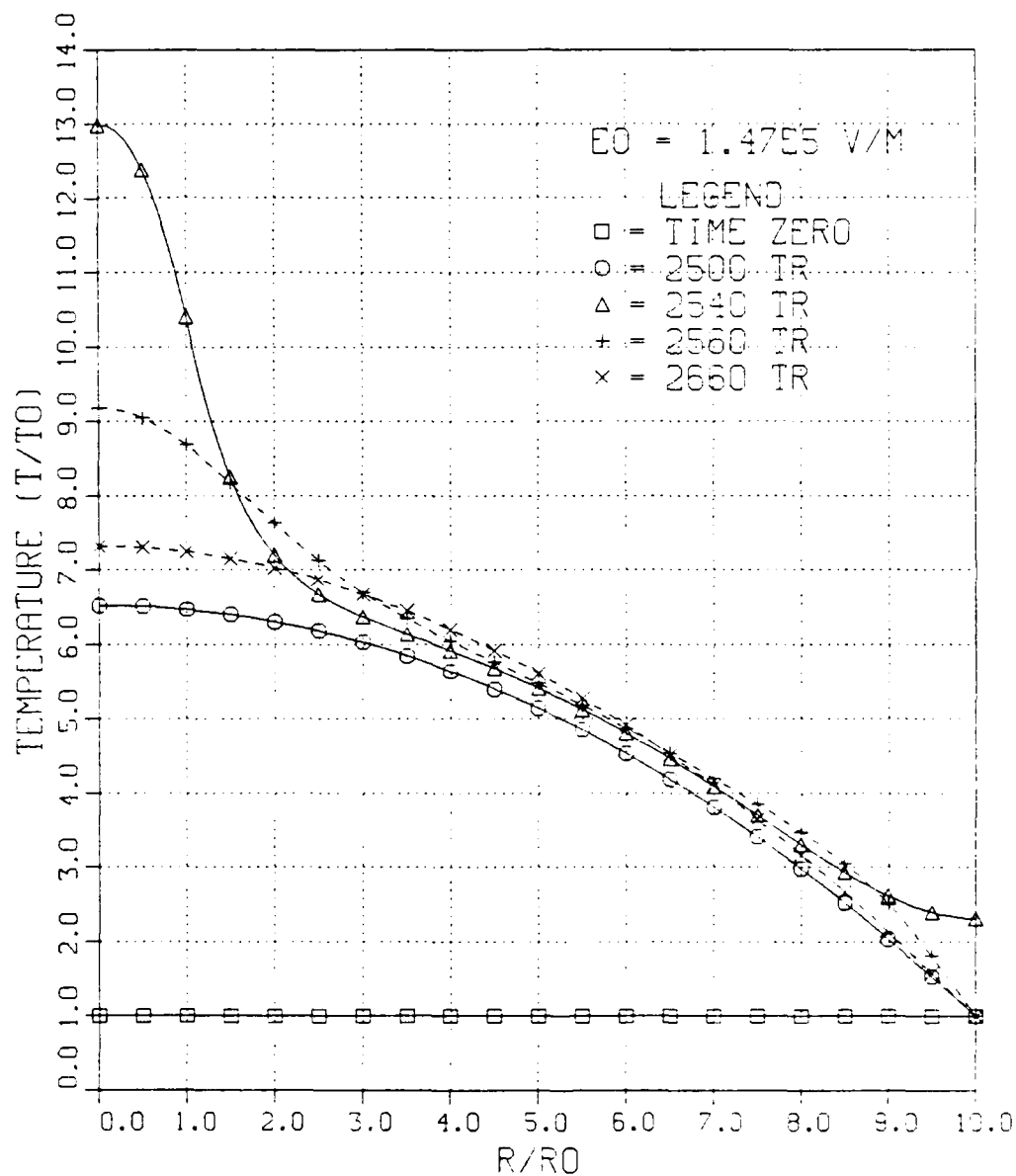


FIGURE 3.26

TEMPERATURE PROFILE
WITH STREAMER ON 45 TR

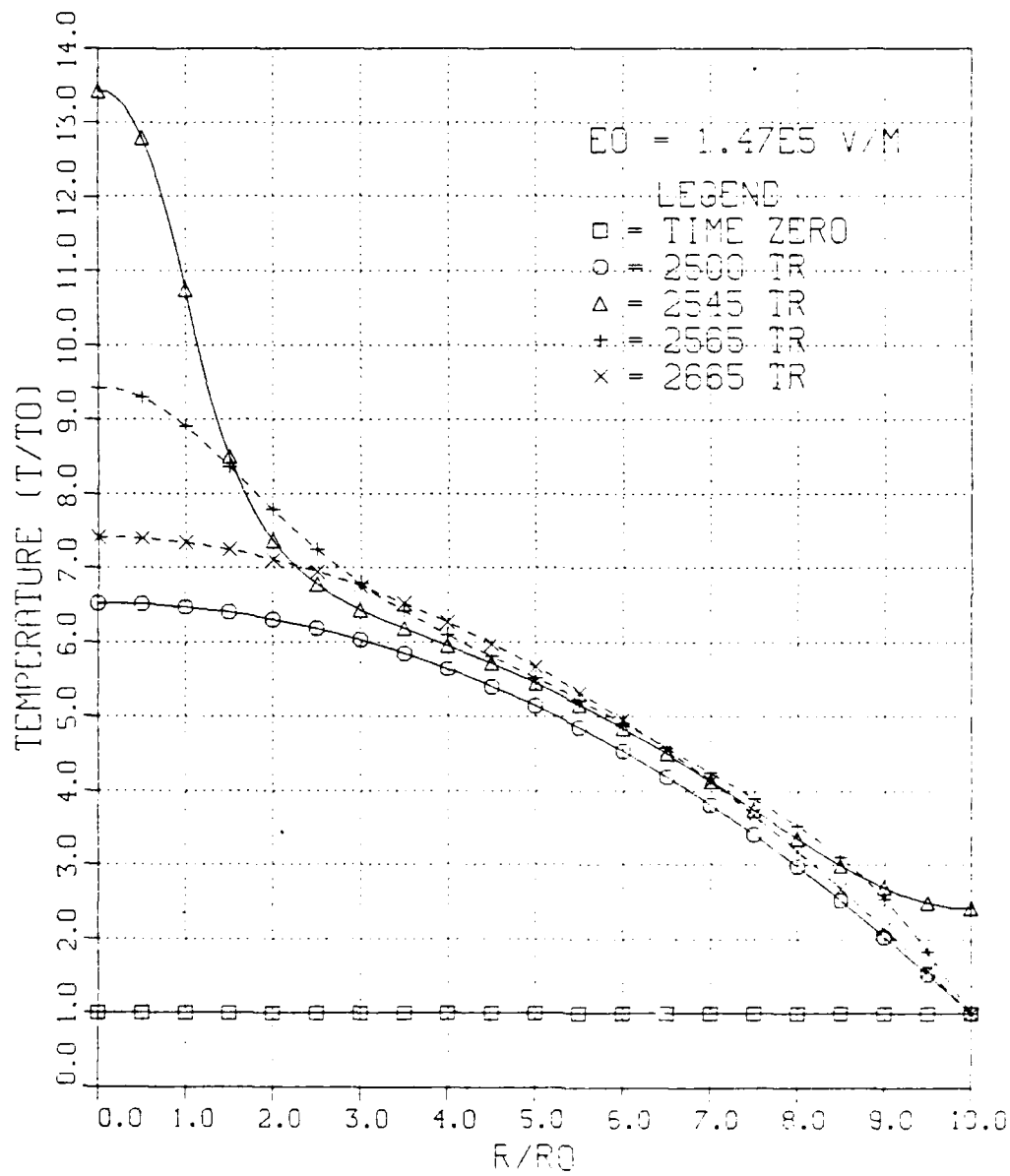


FIGURE 3.27

TEMPERATURE PROFILE
WITH STREAMER ON 50 TR

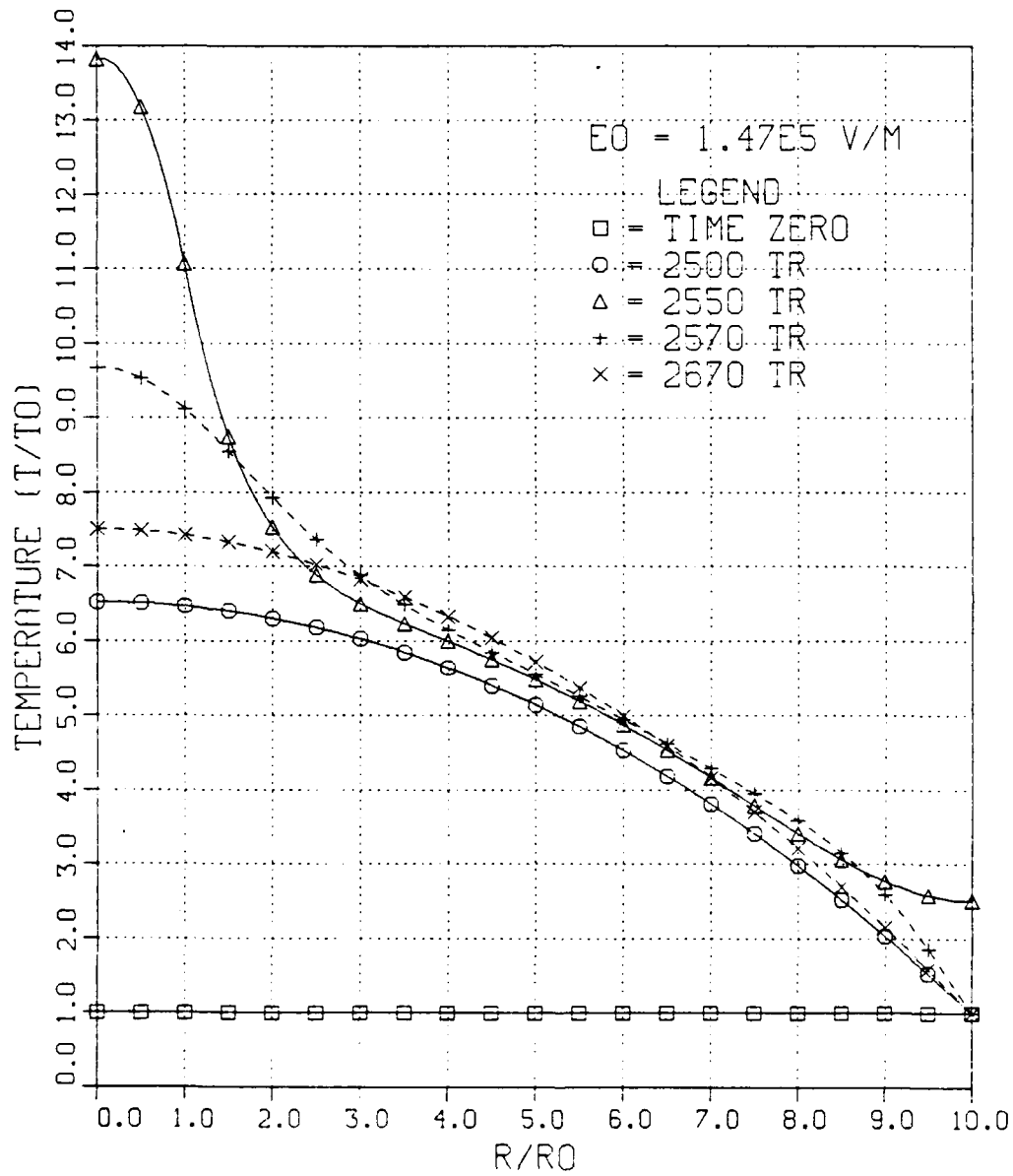


FIGURE 3.28

the streamer. Note that the centerline temperature drops to about half of the rise value in only 20TR and has nearly reached steady state in another 100TR.

Figures 3.29 and 3.30 show a case for a higher E/N value of $7.0\text{E-}17 \text{ V-cm}^2$. Here the steady state temperature profile has a centerline value of about 10.0 and then a streamer "on time" of only 8TR sends the profile above 4000°K . Cases for smaller E/N values produce lower steady state temperature profiles. The streamer effects are similar except that much longer "on times" are needed to produce much of a temperature rise. This appears consistent in the model since at the lower temperature it would take a much larger perturbation to upset the steady state condition, while at the higher energy levels a comparatively smaller perturbation is all that is required.

TEMPERATURE PROFILE
WITH STREAMER ON 5 TR

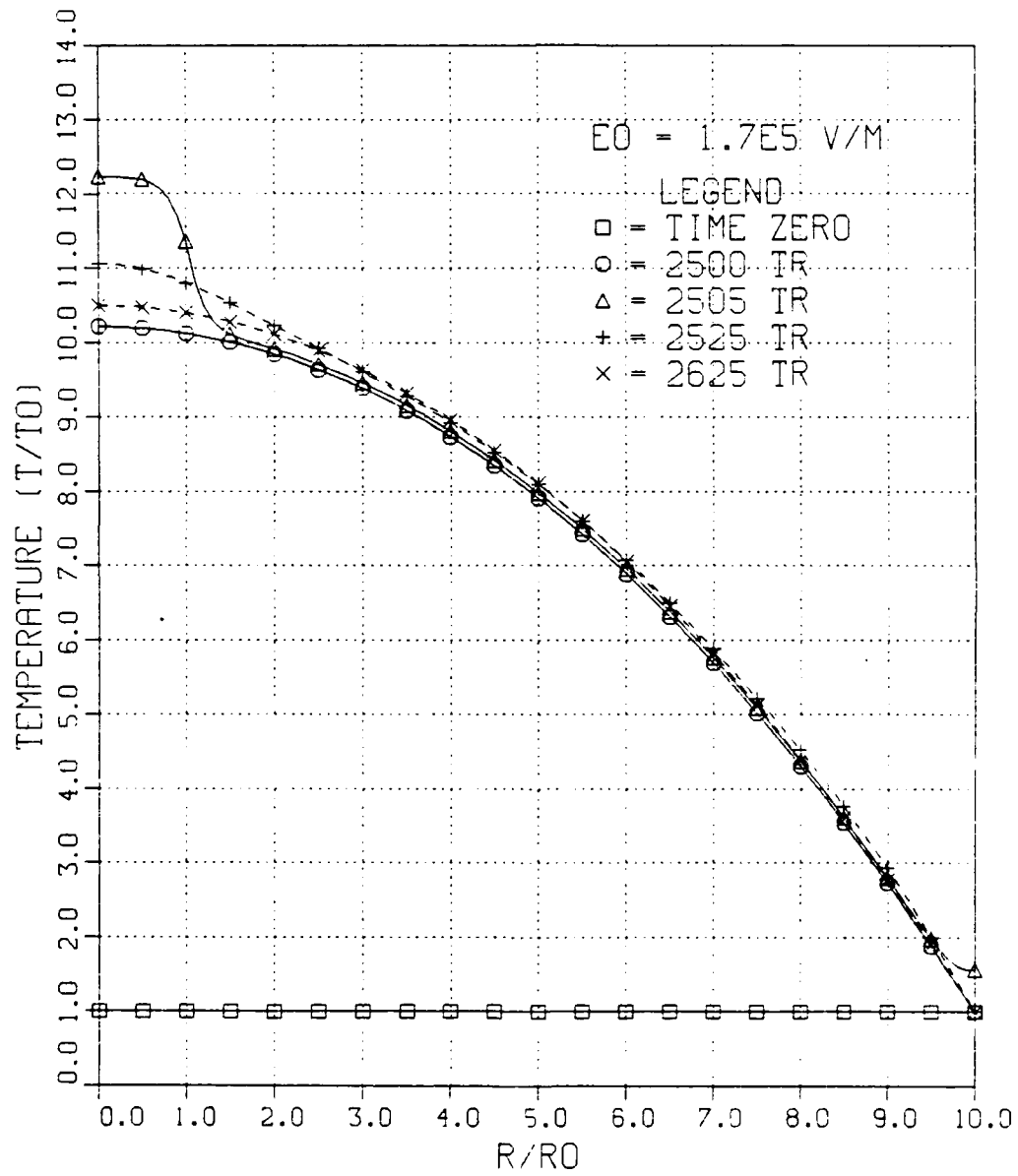


FIGURE 3.29

TEMPERATURE PROFILE
WITH STREAMER ON 9 TR

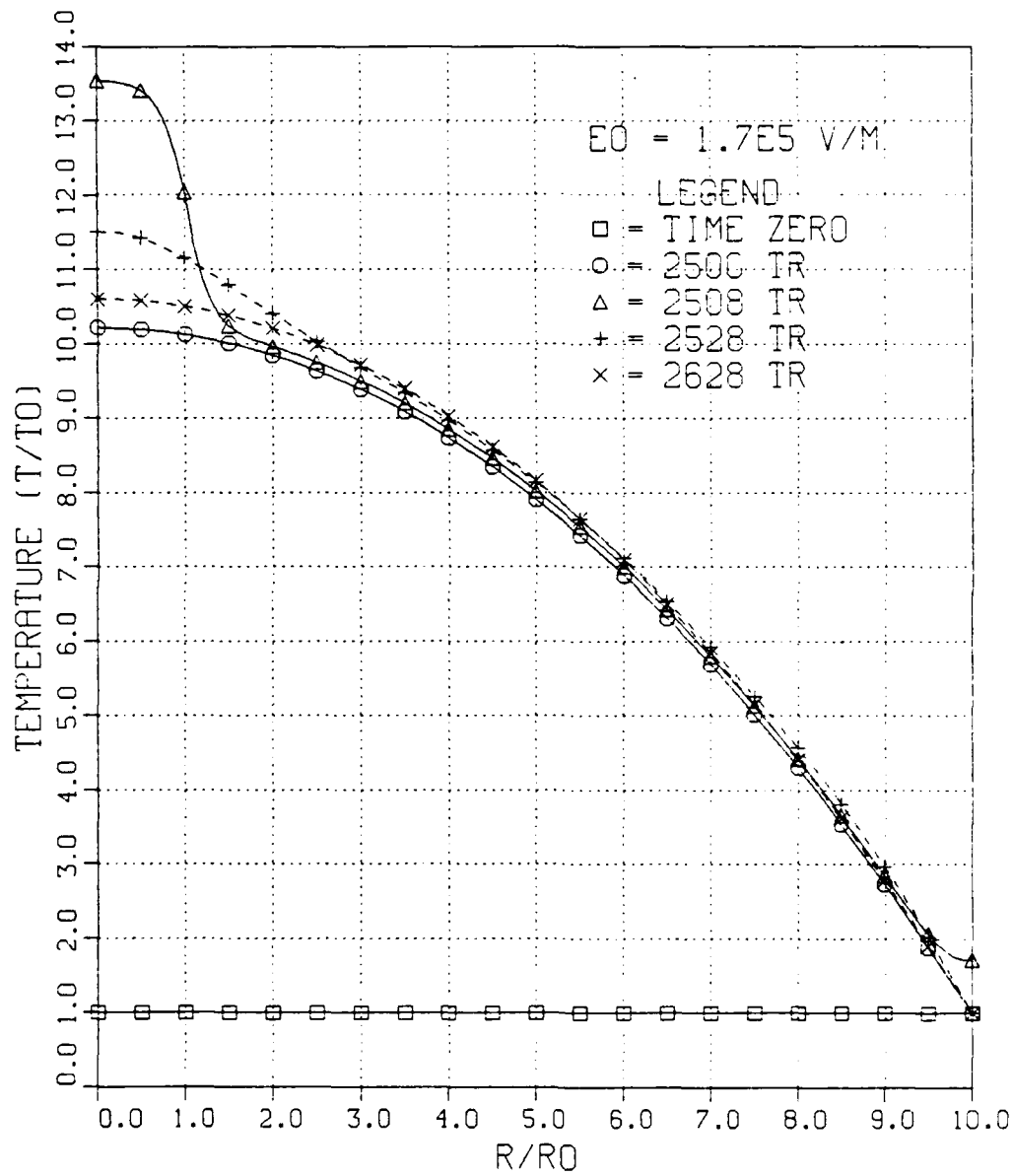


FIGURE 3.30

IV. CONCLUSIONS AND RECOMMENDATIONS

This thesis presents a mathematical model for describing the effects of varying levels of turbulence on glow discharge phenomena. The development is concerned only with the aftereffects of the streamer, rather than its propagation. The program that is presented in Appendix A is intended to allow the investigation of a large variety of cases of interest relating to the glow discharge. The cases discussed in the results chapter are those that appeared to develop a logical sequence of thought in attempting to answer the question of how turbulent gas flows can and do affect the stability of a glow discharge and the problem of delaying the glow-to-arc transition.

The results clearly show that the modelled turbulent flow does indeed have strong beneficial effects on the stability of the system. Additionally, the mathematical model successfully predicts within a reasonable level of uncertainty a region of stability that is consistent with the normal operating ranges of, say, an electrically pumped gas laser [Ref. 10]. The model suggests that the region for which the system maintains thermal stability is critically dependent on E/N . The research showed that a steady state temperature increase from 1200°K to 3000°K results from an increase in E/N of only $5.0E-17$ V-cm² to $7.0E-17$ V-cm².

One important question still remains however. That is; is there a particular level of turbulence which would have the most beneficial effect on the streamer-initiated breakdown problem? This work suggests that the best situation is simply that the most desirable level is the highest level that can be maintained. However, the non-linear nature of the equations suggests that some optimal level may exist [Ref. 2]. Experimental work is probably the best means of answering this question.

The results presented here by no means exhaust the aspects of this problem that could be investigated. The intent of the program is that it can be used as a tool to analyze any desired case. Some logical next steps might be to expand on the streamer modeling aspects to investigate what happens when a follow-on streamer appears before the initial one has fully decayed back to the steady state condition. The "Z" and "Z_A" arrays could be set up to have two or more streamers appear at any desired location. Also, the values of "Z" and "Z_A" used in this model are somewhat arbitrary and probably have to be specified for each individual E/N case according to experimental observation. More research into the actual magnitude of the electric field perturbation may allow the model to more accurately predict the areas of instability with streamer on times that are more in agreement with experiment [Ref. 5].

Mathematically, the analysis of this problem consists of solving the continuity equation for three cases. The first

is for the RHS of Equation (3.4) equal to less than zero. This is the non-ionized environment case. The second is for the RHS equal to zero. This is the steady state case which is what was applied to the ionized environment cases discussed. The third case, which was not applied in this thesis, is for the RHS of the continuity equation to be greater than zero. Investigation into this third case could possibly clarify some aspects of the problem. And finally, the energy equation may have eigenvalue solutions which might produce results of interest such as additional regions of stability.

LIST OF REFERENCES

1. Biblarz, O., Barto, J.L. and Post, H.A., "Gas Dynamic Effects on Diffuse Electrical Discharges in Air," Isreal Journal of Tehnology, v. 15, pp. 59-69, 1977.
2. Wallace, R.J., An Effect of Turbulent Diffusion on the Glow Discharge-To-Arc Transition, Master's Thesis, Naval Postgraduate School, March 1978.
3. Tharratt, C.E., "The Propulsive Duct," Aircraft Engineering, November 1965.
4. Chen, F., Introduction to Plasma Physics, Plenum Press, New York, 1974.
5. Avco Everett Research Laboratory, AFAPL-TR-79-2059, Investigation of the Production of High Density Uniform Plasmas, by D.H. Douglas-Hamilton and P. Rostler, May 1979.
6. Gerald, C.F., Applied Numerical Analysis, Second Edition, Addison-Wesley Publishing Company, Reading, Massachusetts, 1980.
7. Rubchinski, A.V., "Recovery of Breakdown Strength After A Spark Discharge," Investigations Into Electrical Discharges In Gases, Pergamon Press, 1964.
8. Jaeger, E.F., Oster, L. and Phelps, A.V., "Growth of Thermal Constrictions in a Weakly Ionized Gas Discharge in Helium," Physics of Fluids, v. 19, No. 6, p. 819, June 1976.
9. Abramowitz, M. and Stegrin, I.A., Handbook of Mathematical Functions, National Bureau of Standards, 1964.
10. Avco Everett Research Laboratory, AFWL-TR-74-216, Carbon-Dioxide Electric Discharge Laser Kinetics Handbook, by D.H. Douglas-Hamilton and R.S. Lowder, April 1975.

APPENDIX A
THE CHARGE PROGRAM

The Fortran program "CHARGE" is intended to be a working tool for analyzing the glow discharge problem. It evolved from a previously written program which solved the non-linear continuity equation (2.1) [Ref. 2]. It is now arranged in a somewhat different form. The program consists of a main program section which calls up any needed combination of the seven subroutines which perform the desired tasks. As currently written, it can compare four separate cases plus it will display the initial conditions of either the charged particle distribution or the temperature profile. Individual test cases are set up by commenting out (placing a "C" in column 1) those commands not desired. After the main program, there are two sections. The first provides commands to print out the data and the second provides commands to plot the results by utilizing the "DISSPLA" system developed by the Integrated Software Systems Corporation, San Diego, California.

The program as it appears following this discussion is set up to produce the plot displayed in Figure 3.28. The main program begins by defining all arrays. For this example the arrays are set to 101 in the "i" direction which specifies the size of the array with respect to radial position. Since one DR, one radial step, is equal to $r_0/10$,

position "101" specifies a distance of $10 r_0$ perpendicular from the centerline of the streamer. The "j" size is always kept at 2 due to the computing scheme used in the subroutines. After setting the array size, set the variable named "RADIUS" equal to the same value as the "i" coordinate above. In this case, $RADIUS = 101$. This determines how far in the radial direction that the differentiation is to procede. Next one must assign the desired values for BETA and BETAA depending on the case at hand. The BMIN, BMAX, BAMIN and BAMAX parameters apply when it is desired to transition the calculation from a laminar to a turbulent environment. This feature is designed to attempt to ensure that the calculation accounts for the fact that the streamer initially appears so quickly that the flow looks laminar to the streamer no matter what the level of turbulence is. Then, after a period of time, the charged particle distribution left behind by the streamer has existed for sufficient time to now "see" the turbulent effects. The time required for this transition is estimated by noting that the characteristic diffusion time for laminar flow is approximately 0.1 msec [Ref. 2]. Depending on the case at hand, one DT is on the order of a few microseconds. Then, 100 DT (10TR) is on the order of a few tenths of a millisecond. Therefore, for most cases, a transition of 100 DT is used.

Returning to the example, one procedes by selecting the desired initial conditions. In this example, all of the

"N1" values are commented out since they apply to the Bessel function initial condition profile. Four series of subroutine calls are provided then to allow running of four separate cases. Each case assigns its respective results to the "VALX" (X = 0,1,2,3,4...) array for plotting later.

The initial conditions are assigned to VALO or VALTO. Then the first subroutine call will see the initial distribution values of n while each successive call will see the results of the previous call. If it is desired to recover the initial conditions, call either "NZERO" or "TZERO" as desired and the current values will then be reset to time zero.

For this example now, "VAL1" is the result of two calls. The first is for "TRNSTY" to transition from laminar to turbulent conditions with time set to 101, then "DENSTY" is called and runs for 23,900 DT. The result is the steady state temperature distribution in turbulent flow at 2500TR. VAL2 is then the result of calling up the subroutine "STREMR" and running it for 500 DT with BETA and BETAA set to the laminar values. VAL3 then results from calling up "TRNSTY" for 100 DT and "DENSTY" for an additional 100 DT at the turbulent values. Finally, VAL4 simply runs "DENSTY" for another 1000 DT in turbulent conditions to check the decaying temperature profile. Of course, any combination of these subroutine calls and time values can be selected to view the situation as desired.

The results can then be printed out and/or plotted. To become familiar with the "DISSPLA" plot system, refer to DISSPLA Pocket Guide (current with version 9.0) by ISSCO Graphics, 10505 Sorrento Valley Rd, San Diego, California.

Some pointers of potential errors should be clarified. When selecting the desired heading lines, ensure that the last entry in the call to "HEADIN" correctly indicates the total number of heading lines. If no heading appears, this is probably the reason. Secondly, ensure that the third entry in the call to "CURVE" is equal to the "i" value on the arrays. This is the number of points (101 here) to be plotted. And finally, the second entry in the call to "LEGEND" is the number of lines of legend needed, 5, in this example.

The subroutines "DENSTY," "STREMR" and "TRNSTY" all contain essentially the same algorithm with modifications to perform their particular function. The basic idea here is that the calculation proceeds from the first row of data and fills the second row with updated values. Then the first row of old data is replaced by the second row of new data by "SWITCH" and the loop increments one DT and proceeds. With this scheme the program can be run as long as desired without using large values of memory storage.

The boundary conditions for the problems are met by the routine. The left boundary condition assumes that the slope is zero across the streamer centerline. So here, the new

value at $\hat{n}(2,2)$ is assigned to $\hat{n}(1,2)$ before the switch. The right boundary assumes that n is zero at the wall, that is station 101. This is met by limiting the maximum radius value to be one less than "RADIUS" (called "TEMRAD"). The routine proceeds to "TEMRAD," then the last point seen by the calculation algorithm is zero. Similarly, the temperature of the right boundary is set to 1.0.

To compute the conductance parameter, gamma, that would result from any particular \hat{n} distribution, call "CNDUCT" after assigning the desired \hat{n} distribution to some "VALX." The single value "NN" will be returned, which is gamma.

It is hoped that the program is sufficiently self-explanatory. All variable, constant and subroutine names are defined and documentation comments are provided.

CHAOCC10
CHAOCC20
CHAOCC30
CHAOCC40
CHAOCC50
CHAOCC60
CHAOCC70
CHAOCC80
CHAOCC90
CHAOCC100
CHAOCC110
CHAOCC120
CHAOCC130
CHAOCC140
CHAOCC150
CHAOCC160
CHAOCC170
CHAOCC180
CHAOCC190
CHAOCC200
CHAOCC210
CHAOCC220
CHAOCC230
CHAOCC240
CHAOCC250
CHAOCC260
CHAOCC270
CHAOCC280
CHAOCC290
CHAOCC300
CHAOCC310
CHAOCC320
CHAOCC330
CHAOCC340
CHAOCC350
CHAOCC360
CHAOCC370
CHAOCC380
CHAOCC390
CHAOCC400
CHAOCC410
CHAOCC420
CHAOCC430
CHAOCC440
CHAOCC450
CHAOCC460
CHAOCC470
CHAOCC480

THIS PROGRAM MODELS THE EFFECTS OF TURBULENT GAS FLOW ON THE STABILITY OF A GLOW DISCHARGE BREAKDOWN STREAMER. TO ACCOMPLISH THIS, THE PROGRAM CALCULATES THE CHARGED PARTICLE DENSITY AND TEMPERATURE PROFILES FOR AN ELECTRIC DISCHARGE IN A FLOWING GAS ENVIRONMENT. THE PROGRAM USES A FINITE DIFFERENCE SCHEME TO NUMERICALLY SOLVE A CONTINUITY EQUATION TO DETERMINE THE CHARGED PARTICLE DENSITY DISTRIBUTION THEN USES A TRAPEZOIDAL NUMERICAL INTEGRATION SCHEME TO DETERMINE THE CONDUCTANCE. ADDITIONALLY, THE PROGRAM SIMULTANEOUSLY SOLVES AN ENERGY EQUATION UTILIZING THE CALCULATED DENSITY VALUES TO DETERMINE THE TEMPERATURE PROFILE IN THE GAS. IN THE IMMEDIATE REGION OF THE ELECTRIC DISCHARGE IN THE STREAMER, AND FINALLY, TO MODEL THE STREAMER, A MOMENTUM PERTURBATION OF THE ELECTRIC FIELD OVER A RADIAL DISTANCE FROM THE STREAMER CENTERLINE IS INTRODUCED AND THEN THE RESULTING REACTION OF THE SYSTEM IS OBSERVED. BEEN NON-DIMENSIONALIZED.

W.R. OKER - APRIL 1984

NAVAL POSTGRADUATE SCHOOL, MONTEREY, CALIFORNIA

* DEFINITIONS OF VARIABLE AND CONSTANT NAMES *

N = NORMALIZED CHARGED PARTICLE DENSITY (N = N/NO)
NO = N RESULT OF INTEGRATION, EQUALS THE CONDUCTANCE WHEN
NN = MULTIPLIED BY A CONSTANT, EQUAL TO GAMMA IN THE TEXT.
N1 = BESSEL FUNCTION INITIAL CONDITION PROFILE FOR N/NO
T = NORMALIZED TEMPERATURE (T = T/T0), T0 = 300 DEGREES KELVIN
DA = AMBIPOLAR DIFFUSION COEFFICIENT
RADIUS = SPECIFIES RADIAL DISTANCE FROM STREAMER CENTERLINE
R = RADIUS VALUE FOR EACH CALCULATION STEP
RO = RADIUS OF ELECTRIC STREAMER AT TIME ZERO
RHATO = "R" COORDINATE OF RO
RHATI = RHATO + 1
R1 = RADIUS VALUE FOR EACH CALCULATION STEP USED BY CONDUCTANCE
CUNRAD = SPECIFIES RADIAL DISTANCE FROM STREAMER CENTERLINE FOR
TEMRAD = CALCULATING THE CONDUCTANCE OUT TO A SPECIFIED RADIUS
A2 = TWC-BODY RECOMBINATION COEFFICIENT
A3 = THREE-BODY RECOMBINATION COEFFICIENT
TIME = DETERMINES NUMBER OF TIME STEPS TO BE USED FOR CALCULATION

CC

CHAO0C490
CHAO0C500
CHAO0C510
CHAO0C520
CHAO0C530
CHAO0C540
CHAO0C550
CHAO0C560
CHAO0C570
CHAO0C580
CHAO0C590
CHAO0C600
CHAO0C610
CHAO0C620
CHAO0C630
CHAO0C640
CHAO0C650
CHAO0C660
CHAO0C670
CHAO0C680
CHAO0C690
CHAO0C700
CHAO0C710
CHAO0C720
CHAO0C730
CHAO0C740
CHAO0C750
CHAO0C760
CHAO0C770
CHAO0C780
CHAO0C790
CHAO0C800
CHAO0C810
CHAO0C820
CHAO0C830
CHAO0C840
CHAO0C850
CHAO0C860
CHAO0C870
CHAO0C880
CHAO0C890
CHAO0C900
CHAO0C910
CHAO0C920
CHAO0C930
CHAO0C940
CHAO0C950
CHAO0C960

```

CT = DELTA T FOR DENSITY CALCULATION (TIME STEP)
DTA = DELTA T FOR TEMPERATURE CALCULATION
DR = DELTA R (RADIUS STEP)
ALPHA = ACN-DIMENSIONALIZED RECOMBINATION COEFFICIENT
BETA = FLUX CONDITION PARAMETER (DEGREE OF LAMINAR OR
TURBULENT CONDITION) FOR DENSITY CALCULATION
BETAA = SAME AS BETA FOR TEMPERATURE CALCULATION
BMIN = BETA AT END OF TRANSITION TO TURBULENT CONDITIONS
BMAX = BETA AT BEGINNING OF TRANSITION FROM LAMINAR TO
TURBULENT CONDITION
BAPIN = BMIN FOR TEMPERATURE CALCULATION
EAPAX = BMAX FOR TEMPERATURE CALCULATION
RR = R/FO ARRAY (FOR PLOTTING)
VALT.X = N VALUE ARRAY (FOR PLOTTING)
VALT.X = T VALUE ARRAY (FOR PLOTTING)
EO = INITIAL VELOCITY CHARGED PARTICLE STRENGTH (FOR REFERENCE, NOT USED
FOR CALCULATION PURPOSES)
Z = MULTIPLIER FOR CHARGED PARTICLE DENSITY VALUE TO SIMULATE
THE ELECTRIC FIELD PERTURBATION INTRODUCED BY THE STREAMER
ZA = SAME AS "Z" BUT FOR TEMPERATURE VALUE

*****
* LIST OF SUBROUTINES *
*****

NZERO = INITIALIZES CHARGED PARTICLE DENSITY PROFILE
TZERO = INITIALIZES TEMPERATURE PROFILE
SWITCH = REPLACES "FIRST ROW" DATA WITH COMPUTED "SECOND
ROW" DATA FOR COMPUTATION ALGORITHM SCHEME
DENSITY = CALCULATES CHARGED PARTICLE DENSITY AND
TEMPERATURE VALUES
STREMR = INTRODUCES ELECTRIC FIELD PERTURBATION TO MODEL
EFFECT OF STREAMER
TRANSTY = SAME AS DENSITY EXCEPT THAT IT ALLOWS FOR A TRANSITION
FROM LAMINAR TO TURBULENT FLOW
CNDUCT = COMPUTES GAMMA FROM AN INPUT
CHARGED PARTICLE DENSITY PROFILE

*****
* SET UP SUBROUTINE TO DEFINE INITIAL CONDITIONS FOR CHARGED *
* PARTICLE DENSITY PROFILE *
*****
*****
SUBROUTINE NZERO(N,RADIUS,RHATO)
DOUBLE PRECISION N(RADIUS,2)
INTEGER I,RADIUS,RHATO,RHATI
RHATI = RHATO +

```

CHAO1C570
CHAO1C580
CHAO1C590
CHAO1C600
CHAO1C610
CHAO1C620
CHAO1C630
CHAO1C640
CHAO1C650
CHAO1C660
CHAO1C670
CHAO1C680
CHAO1C690
CHAO1C700
CHAO1C710
CHAO1C720
CHAO1C730
CHAO1C740
CHAO1C750
CHAO1C760
CHAO1C770
CHAO1C780
CHAO1C790
CHAO1C800
CHAO1C810
CHAO1C820
CHAO1C830
CHAO1C840
CHAO1C850
CHAO1C860
CHAO1C870
CHAO1C880
CHAO1C890
CHAO1C900
CHAO1C910
CHAO1C920
CHAO1C930
CHAO1C940
CHAO1C950
CHAO1C960
CHAO1C970
CHAO1C980
CHAO1C990
CHAO1C1000
CHAO1C1010
CHAO1C1020
CHAO1C1030
CHAO1C1040
CHAO1C1050
CHAO1C1060
CHAO1C1070
CHAO1C1080
CHAO1C1090
CHAO1C1100
CHAO1C1110
CHAO1C1120
CHAO1C1130
CHAO1C1140
CHAO1C1150
CHAO1C1160
CHAO1C1170
CHAO1C1180
CHAO1C1190
CHAO1C1200
CHAO1C1210
CHAO1C1220
CHAO1C1230
CHAO1C1240
CHAO1C1250
CHAO1C1260
CHAO1C1270
CHAO1C1280
CHAO1C1290
CHAO1C1300
CHAO1C1310
CHAO1C1320
CHAO1C1330
CHAO1C1340
CHAO1C1350
CHAO1C1360
CHAO1C1370
CHAO1C1380
CHAO1C1390
CHAO1C1400
CHAO1C1410
CHAO1C1420
CHAO1C1430
CHAO1C1440

```

DO 10 I = 1,RHATO
  N(I,1) = 1.0
  N(I,2) = 1.0
1C CONTINUE
DO 20 I = R+1,RADIUS
  N(I,1) = 0.0
  N(I,2) = 0.0
2C CONTINUE
RETURN
END

*****
** SET UP SLEROUTINE TO DEFINE INITIAL CONDITIONS FOR TEMPERATURE **
** PROFILE *****
*****
SUBROUTINE TZERC(T,RADIUS)
DOUBLE PRECISION T(RADIUS,2)
INTEGER I,RADIUS
DO 25 I = 1,RADIUS
  T(I,1) = 1.0
  T(I,2) = 1.0
25 CONTINUE
RETURN
END

*****
** SET UP SLEROUTINE TO SWITCH COMPUTED DENSITY AND TEMPERATURE **
** VALUES FROM SECOND ROW BACK TO FIRST ROW FOR NEXT CALCULATION **
** SEQUENCE *****
*****
SUBROUTINE SWITCH(N,T,RADIUS)
DOUBLE PRECISION N(RADIUS,2),T(RADIUS,2)
INTEGER I,RADIUS
DO 30 I = 1,RADIUS
  N(I,1) = N(I,2)
  T(I,1) = T(I,2)
30 CONTINUE
RETURN
END

*****
** SET UP SLEROUTINE TO CALCULATE CHARGED PARTICLE DENSITY VALUES **
** AND TEMPERATURE PROFILE FOR ANY ARBITRARY BETA AND/OR BETA **
** VALUE *****
*****

```



```

C * VALUE DUE TO PERTURBATION OF ELECTRIC FIELD BY STREAMER *
C *****
C SUBROUTINE STREAMR(TIME,RADIUS,I,N,BETA,BETA1,N1,Z,ZA)
C DOUBLE PRECISION A,B,C,N(RADIUS,2),NO,A2,A3,DT,DR,ALPHA,BETA,R,
C *T(RADIUS,2),BETAA,C,E,DTA,N(RADIUS,2),Z(RADIUS),Z(RADIUS)
C INTEGER I,J,K,TIME,RADIUS,TEMRAD
C TEMRAD = RADIUS - 1
C NO = 8.20E16
C A2 = 1.E-13
C A3 = 1.E-35
C CT = 0.1
C DTA = 1.057E-3
C DR = 0.1
C ALPHA = (A3*NO)/A2
C DO GO K = 1,TIME
C CALL SWITCH(N,I,RADIUS)
C DO 74 I = 2,TEMRAD
C J = 1
C R = (FLOAT(I)-1)/10.
C A = (1./(DR*DR))*N(I+1,J)-(2.*N(I,J))+N(I-1,J))
C E = (1./(2.*R*DR))*N(I+1,J)-N(I-1,J))
C C = N(I,J)*N(I,J)+ALPHA*N(I,J)**3.
C *****
C * USE FOLLOWING VALUE FOR C. IF IONIZATION TERM DESIRED *
C *****
C C = N(I,J)*N(I,J)+ALPHA*N(I,J)**3.-Z(I)*N(I,J)
C E = (1./(DR*DR))*N(I+1,J)-(2.*N(I,J))+N(I-1,J))
C E = (1./(2.*R*DR))*N(I+1,J)-N(I-1,J))
C N(I,J+1) = (DT*((1./BETA)*(A+E))-C)*N(I,J)
C T(I,J+1) = DTA*((1./BETAA)*(D+E)+Z(I)*N(I,J))+T(I,J)
C IF (N(I,J+1)).GT.1.E-14) GO TO 74
C CONTINUE
C IF (I.NE.2) GO TO 75
C T(I-1),(J+1) = N(I,(J+1))
C T(I-1),(J+1) = T(I,(J+1))
C CONTINUE
C IF (I.NE.TEMRAD) GO TO 76
C T(I+1),(J+1) = T(I,(J+1))
C CONTINUE
C CONTINUE
C RETURN
C ENC
C

```

```

CHA01530
CHA01540
CHA01550
CHA01560
CHA01570
CHA01580
CHA01590
CHA02000
CHA02010
CHA02020
CHA02030
CHA02040
CHA02050
CHA02060
CHA02070
CHA02080
CHA02090
CHA02100
CHA02110
CHA02120
CHA02130
CHA02140
CHA02150
CHA02160
CHA02170
CHA02180
CHA02190
CHA02200
CHA02210
CHA02220
CHA02230
CHA02240
CHA02250
CHA02260
CHA02270
CHA02280
CHA02290
CHA02300
CHA02310
CHA02320
CHA02330
CHA02340
CHA02350
CHA02360
CHA02370
CHA02380
CHA02390
CHA02400

```



```

C C C C C C C C C C
8C CONTINUE
RETURN
ENC

*****
** SET UP SLERCUTINE TO COMPUTE THE CONDUCTANCE PARAMETER **
** GAMMA BY INTEGRATION *****
*****

SUBROUTINE CNDUCT(RADILS,NN,VALX,R1)
REAL NA,VALX(RADIUS),R1(RADIUS),SUM,DR,FI
INTEGER J,RADIUS
DR = 0.1
NN = 0.0
PI = 3.141592654
DO 50 J = 2,RADIUS
    SUM = PI*((R1(J)*VALX(J)+(R1(J-1))*VALX(J-1)))*DR
    NN = NN + SUM
50 CONTINUE
RETURN
ENC

*****
** MAIN PROGRAM BEGINS **
*****

REAL RR(101),VALO(101),VALT1(101),VALT2(101),VALT3(101),VAL4(101),
VALTO(101),VALTI(101),VALT N(101,2),BETA,BMIN,BMAX,T(101,2),BETAA,
*N1(101,2),BAMIN,BAMAX,Z(101),ZA(101)
REAL NN,N1(101),N1,NNAZ,NNZ,NN4,E0
INTEGER I,TIME,RADILS,CNCRAD,RHATO,RHAT1,RSTRMO,RSTRM1

*****
** INITIALIZE VALUES *
*****

BETA = 66.560000
BMIN = 23.6300
BMAX = 66.5600
BETAA = 0.62520
BAMIN = 0.22190
BAMAX = 0.62520
EO = 1.468EE1
RADLIUS = 101
RHATO = 11
RHAT1 = RHATO + 1
RSTRMO = 11
RSTRM1 = 11

```

```

RSTRM1 = RSTRMO + 1
CONRAD = 11
DO 50 I = 1, RSTRMO
  Z(I) = 1C.0
  ZA(I) = 2.5
5C CONTINUE
DO 60 I = RSTRM1, RADIUS
  Z(I) = 1.0
  ZA(I) = 1.0
6C CONTINUE
DO 100 I = 1, RHATO
  N(I,1) = 1.0
  N(I,2) = 1.0
10C CONTINUE
DO 110 I = RHAT1, RADIUS
  N(I,1) = 0.0
  N(I,2) = 0.0
11C CONTINUE
DO 12C I = 1, RADIUS
  T(I,1) = 1.0
  T(I,2) = 1.0
12C CONTINUE
N1(1,1) = 1.00000
N1(2,1) = 0.99750
N1(3,1) = 0.99376
N1(4,1) = 0.99002
N1(5,1) = 0.98382
N1(6,1) = 0.97762
N1(7,1) = 0.96501
N1(8,1) = 0.96039
N1(9,1) = 0.94943
N1(10,1) = 0.93846
N1(11,1) = 0.92523
N1(12,1) = 0.91200
N1(13,1) = 0.89660
N1(14,1) = 0.88120
N1(15,1) = 0.86374
N1(16,1) = 0.84628
N1(17,1) = 0.82690
N1(18,1) = 0.80752
N1(19,1) = 0.78636
N1(20,1) = 0.76519
N1(21,1) = 0.74241
N1(22,1) = 0.71962
N1(23,1) = 0.69538
N1(24,1) = 0.67113
N1(25,1) = 0.64561
N1(26,1) = 0.62008

```

```

CCCCCCCCCCCCCCCCCCCCCCCCCCCCCCCC

```

```

CHAO 370
CHAO 380
CHAO 390
CHAO 400
CHAO 410
CHAO 420
CHAO 430
CHAO 440
CHAO 450
CHAO 460
CHAO 470
CHAO 480
CHAO 490
CHAO 500
CHAO 510
CHAO 520
CHAO 530
CHAO 540
CHAO 550
CHAO 560
CHAO 570
CHAO 580
CHAO 590
CHAO 600
CHAO 610
CHAO 620
CHAO 630
CHAO 640
CHAO 650
CHAO 660
CHAO 670
CHAO 680
CHAO 690
CHAO 700
CHAO 710
CHAO 720
CHAO 730
CHAO 740
CHAO 750
CHAO 760
CHAO 770
CHAO 780
CHAO 790
CHAO 800
CHAO 810
CHAO 820
CHAO 830
CHAO 840

```



```

C      CALL TRANSY(000101,RADIUS,I,N,BMIN,EMAX,BAMIN,BAMAX,N1)
C      CALL DENSITY(024900,RADIUS,T,N,BMIN,EAMIN,N1)
C      DO 400 I = 1,RADIUS
C          VAL1(I) = N(I,1) + 1.E-70
C          VAL2(I) = T(I,1) + 1.E-70
C      CONTINUE
C      CALL NZERG(N,RADIUS,RHATO)
C      CALL TZERG(T,RADIUS)
C      CALL DENSITY(005001,RADIUS,I,N,BMIN,BAMIN,N1)
C      CALL STFERM(000500,RADIUS,I,N,BETA,BETAA,N1,Z,ZA)
C      CALL TRANSY(009000,RADIUS,I,N,5000.,BMAX,BAMIN,BAMAX,N1)
C      CALL DENSITY(010000,RADIUS,T,N,5000.,BAMIN,N1)
C      DO 410 I = 1,RADIUS
C          VAL2(I) = N(I,1) + 1.E-70
C          VAL12(I) = T(I,1) + 1.E-70
C      CONTINUE
C      CALL NZERG(N,RADIUS,RHATO)
C      CALL TZERG(T,RADIUS)
C      CALL DENSITY(005001,RADIUS,I,N,BMIN,BAMIN,N1)
C      CALL STFERM(000100,RADIUS,I,N,BETA,BETAA,N1,Z,ZA)
C      CALL TRANSY(000100,RADIUS,I,N,BMIN,EMAX,BAMIN,BAMAX,N1)
C      CALL DENSITY(000100,RADIUS,T,N,BMIN,EAMIN,N1)
C      DO 420 I = 1,RADIUS
C          VAL3(I) = N(I,1) + 1.E-70
C          VAL13(I) = T(I,1) + 1.E-70
C      CONTINUE
C      CALL NZERG(N,RADIUS,RHATO)
C      CALL TZERG(T,RADIUS)
C      CALL DENSITY(001000,RADIUS,I,N,BMIN,BAMIN,N1)
C      CALL STFERM(000100,RADIUS,I,N,BETA,BETAA,N1,Z,ZA)
C      CALL TRANSY(009000,RADIUS,I,N,50.0,BMAX,BAMIN,BAMAX,N1)
C      CALL DENSITY(010000,RADIUS,T,N,50.0,BETAA,N1)
C      DO 430 I = 1,RADIUS
C          VAL4(I) = N(I,1) + 1.E-70
C          VAL14(I) = T(I,1) + 1.E-70
C      CONTINUE
C      CALL NZERG(N,RADIUS,RHATO)
C      CALL TZERG(T,RADIUS)
C      CALL DENSITY(001000,RADIUS,I,N,BMIN,BAMIN,N1)
C      CALL STFERM(000100,RADIUS,I,N,BETA,BETAA,N1,Z,ZA)
C      CALL TRANSY(010000,RADIUS,I,N,50.0,BMAX,BAMIN,BAMAX,N1)
C      CALL DENSITY(010000,RADIUS,T,N,50.0,BETAA,N1)
C      DO 499 I = 1,RADIUS
C          RI(I) = (FLCAT(I)-1.)/10.
C      CONTINUE
C      CALL CNDUCT(RADIUS,NN,VAL1,RI)
C      NN1 = NN
C      CALL CNDUCT(RADIUS,NN,VAL2,RI)
C      NN2 = NN
C      *****
C      * PERFORM INTEGRATIONS FOR CONDUCTANCE CALCULATIONS *
C      *****

```

```

CHA04430
CHA04440
CHA04450
CHA04460
CHA04470
CHA04480
CHA04490
CHA04500
CHA04510
CHA04520
CHA04530
CHA04540
CHA04550
CHA04560
CHA04570
CHA04580
CHA04590
CHA04600
CHA04610
CHA04620
CHA04630
CHA04640
CHA04650
CHA04660
CHA04670
CHA04680
CHA04690
CHA04700
CHA04710
CHA04720
CHA04730
CHA04740
CHA04750
CHA04760
CHA04770
CHA04780
CHA04790
CHA04800

```


CHAO:170
CHAO:1780
CHAO:190
CHAO:200
CHAO:210
CHAO:220
CHAO:230
CHAO:240
CHAO:250
CHAO:260
CHAO:270
CHAO:280
CHAO:290
CHAO:300
CHAO:310
CHAO:320
CHAO:330
CHAO:340
CHAO:350

CALL CLEVE(RR, VALT2,101,5)
CALL RESET("DASH")
CALL CLEVE(RR, VALT3,101,5)
CALL RESET("DASH")
CALL DASH
CALL CLEVE(RR, VALT4,101,5)
CALL RESET("DASH")
CALL LINES("TIME ZERO",LP,1)
CALL LINES("2500 TR",LP,2)
CALL LINES("2550 TR",LP,3)
CALL LINES("2570 TR",LP,4)
CALL LINES("2670 TR",LP,5)
CALL LEGEND(LP,5,2.8,4.0)
CALL ENDFL(0)
CALL DUNEFL
CALL STCP
CALL ENCL

C
C
C
C

APPENDIX B

HP-41 PROGRAM

In the course of developing the results of Chapter III, it is necessary to perform a large number of simple but tedious calculations. The following HP-41CV program proved helpful. It should be easily adaptable to any small programmable calculator.

The program prompts the user for E/N ($V\text{-cm}^2$), v_i/N (cm^3/s), N (cm^{-3}), α_2 (m^3/s) and v_d (cm/s). These data are available from Figure 2.2.

The program then displays E (V/m), N_0 (m^{-3}), α_2 (m^3/s), DTA, BETAL (laminar), BETAT (turbulent), BETAAL (laminar), BETAAT (turbulent) and DT in true time in microsecs. The minimum BETA values computed are consistent with the stability criterion, Equation (2.17). It is good practice to add about 1% to these values to ensure a smooth running calculation.

01	LBL [Name Program]	37	STO08	73	3.199E-8
02	E/N?	38	RCL04	74	*
03	PROMPT	39	ENTER	75	STO13
04	STO01	40	RCL07	76	RCL10
05	V/N?	41	*	77	ENTER
06	PROMPT	42	1/X	78	RCL12
07	STO02	43	STO09	79	/
08	N?	44	RCL09	80	STO14
09	PROMPT	45	ENTER	81	200
10	STO03	46	10	82	ENTER
11	ALPHA2?	47	/	83	RCL14
12	PROMPT	48	STO10	84	*
13	STO04	49	1.6E-19	85	STO15
14	Vd?	50	ENTER	86	RCL08
15	PROMPT	51	RCL07	87	ENTER
16	STO05	52	*	88	RCL15
17	RCL01	53	RCL05	89	*
18	ENTER	54	*	90	RCL13
19	RCL03	55	RCL06	91	/
20	*	56	/	92	STO16
21	100	57	100	93	RCL06
22	*	58	/	94	E =
23	STO06	59	STO11	95	ARCL X
24	RCL02	60	2.223E5	96	AVIEW
25	ENTER	61	ENTER	97	STOP
26	RCL03	62	RCL11	98	RCL07
27	*	63	/	99	N0 =
28	RCL04	64	RCL06	100	ARCL X
29	/	65	X ⁷ /2	101	AVIEW
30	STO07	66	/	102	STOP
31	RCL04	67	STO12	103	RCL04
32	ENTER	68	RCL11	104	ALPHA2 =
33	RCL07	69	ENTER	105	ARCL X
34	*	70	RCL06	106	AVIEW
35	8E-3	71	X ⁷ /2	107	STOP
36	*	72	*	108	RCL14

AD-A151 838

TURBULENCE EFFECTS ON A GLOW DISCHARGE AS DERIVED FROM
CONTINUITY AND ENERGY CONSIDERATIONS(U) NAVAL
POSTGRADUATE SCHOOL MONTEREY CA W R OKER SEP 84

2/2

UNCLASSIFIED

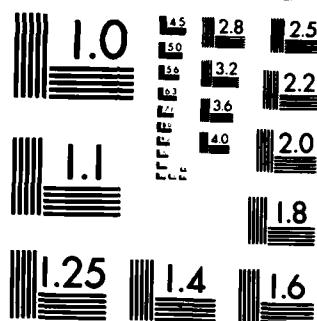
F/G 20/4

NL

END

FORMED

DATE



109 DTA =
110 ARCL X
111 AVIEW
112 STOP
113 RCL08
114 BETAL =
115 ARCL X
116 AVIEW
117 STOP
118 RCL16
119 BETAT =
120 ARCL X
121 AVIEW
122 STOP
123 RCL13
124 BETAAL =
125 ARCL X
126 AVIEW
127 STOP
128 RCL15
129 BETAAT =
130 ARCL X
131 AVIEW
132 STOP
133 RCL10
134 ENTER
135 1E-6
136 /
137 DTT =
138 ARCL X
139 AVIEW
140 END

BIBLIOGRAPHY

- Bekefi, G., Principles of Laser Plasmas, John Wiley & Sons, New York, 1976.
- Chapman, Brian N., Glow Discharge Processes, John Wiley & Sons, New York, 1980.
- Cobine, James D., Gaseous Conductors, Dover Publications, New York, 1958.
- Engel, A. von, Ionized Gases, Oxford at the Clarendon Press, 1965.
- Klyarfel'd, B.N., (Ed.), Investigations into Electric Discharges in Gases, Pergamon Press, New York, 1964.
- Nasser, Essam, Fundamentals of Gaseous Ionization & Plasma Electronics, John Wiley & Sons, New York, 1971.
- Velikhov, E.P., Golubev, V.S. and Pashkin, S.V., "Glow Discharge in a Gas Flow," Soviet Physics, Usp., v. 25(5), May 1982.
- Wasserstrom, E. and Crispin, Y., "Stability of Glow Discharge," Journal of Applied Physics, v. 53, No. 8, pp. 5565-5577, August 1982.

INITIAL DISTRIBUTION LIST

	No. Copies
1. Defense Technical Information Center Cameron Station Alexandria, VA 22314	2
2. Chairman, Code 67 Department of Aeronautics Naval Postgraduate School Monterey, CA 93943	1
3. Library, Code 0142 Naval Postgraduate School Monterey, CA 93943	2
4. Professor O. Biblarz, Code 67Bi Department of Aeronautics Naval Postgraduate School Monterey, CA 93943	6
5. Dr. Alan Garscadden AFAPL/POD Building 450/Room D101 Wright-Patterson AFB, Ohio 45433	1
6. LCDR J.L. Barto, USN Weapons System Officer, Code 2004 Pacific Missile Test Center Point Mugu, CA 93042	1
7. LCDR William R. Oker, USN Naval Air Systems Command (Navair 417) Arlington, VA 20361	1

END

FILMED

4-85

DTIC